# Evaluation of land surface model simulations of evapotranspiration over a 12-year crop succession: impact of the soil hydraulic properties.

Garrigues, Sébastien[1,2]; Olioso Albert[1,2]; Calvet, Jean-Christophe[3]; Martin, Eric[3]; Lafont, Sébastien[5] ; Moulin, Sophie[1,2]; Chanzy, André [1,2]; Marloie, Olivier[4]; Desfonds, Véronique[1,2]; Bertrand, Nadine[1,2]; Renard, Dominique[1,2], Buis, Samuel[1,2].

[1] INRA, UMR1114 EMMAH, F-84914 Avignon Cedex 9, France

[2] Université d'Avignon et des Pays de Vaucluse, UMR1114 EMMAH, F-84000 Avignon, France

[3] CNRM-GAME, UMR3589, Météo-France, CNRS, Toulouse, France

[4] URFM, INRA, Avignon, France

[5] ISPA, INRA, Bordeaux, France

Submitted to Hydrology and Earth System Sciences

## Abstract

Evapotranspiration has been recognized as one of the most uncertain term in the surface water balance simulated by land surface models. In this study, the SURFEX/ISBA-A-gs simulations of evapotranspiration are assessed at the field scale over a 12-year Mediterranean crop succession. The model is evaluated in its standard implementation which relies on the use of the ISBA pedotransfer estimates of the soil properties. The originality of this work consists in explicitly representing the succession of crop cycles and inter-crop bare soil periods in the simulations and assessing its impact on the dynamic of simulated and measured evapotranspiration over a long period of time. The analysis focuses on key soil parameters which drive the simulation of evapotranspiration, namely the rooting depth, the soil moisture at saturation, the soil moisture at field capacity and the soil moisture at wilting point. The simulations achieved with the standard values of the soil parameters derived from the ISBA pedotransfer functions are compared to those achieved with the *in situ* values. Various *in situ* estimates of the soil parameters are tested and the estimates that lead to the most accurate representation of ET dynamic over the crop succession at the field scale are selected. Finally, the impact of uncertainties in in situ soil parameters on ET simulations is evaluated and compared with the uncertainties triggered by a key vegetation parameter (the mesophyll conductance).

This work shows that evapotranspiration mainly results from the soil evaporation when it is continuously simulated over a Mediterranean crop succession. The evapotranspiration simulated with the standard surface and soil parameters of the model is largely underestimated. The deficit in cumulative evapotranspiration amounts to 24% over 12 years. The bias in daily daytime evapotranspiration is -0.24 mm $day^{-1}$. The ISBA pedotransfer estimates of the soil moisture at saturation and at wilting point are overestimated which explains most of the evapotranspiration underestimation. The use of field capacity values derived from laboratory measurements leads to inaccurate simulation of soil evaporation due to the lack of representativeness of the soil structure variability at the field scale. The most accurate simulation is achieved with the average values of the soil properties derived from the analysis of field measurements of soil moisture vertical profiles over each crop cycle. The use of crop-varying values of the soil parameters over the crop succession has little impact on the simulation performances. Finally, we show that the spatiotemporal variability in the soil

parameters generate substantial uncertainties in simulated ET (the 95% confidence interval represents 23% of cumulative ET over 12-years) which are much larger than the uncertainties triggered by variations in the mesophyll conductance. Measurement random errors explain a large part of the scattering between simulations and measurements at half-hourly time scale. The deficits in simulated ET reported in this work are probably larger due to likely underestimation of ET by eddy-covariance measurements. Other possible model shortcomings include the lack of representation of soil vertical heterogeneity and root profile along with inaccurate energy balance partitioning between the soil and the vegetation at low LAI.

**Keys words:**

Land surface model, evapotranspiration, crop succession, soil hydraulic properties, eddy covariance.

## 1 Introduction

Land surface models (LSMs) are relevant tools to analyze and predict the evolution of the water balance at various spatial and temporal scales. They describe water, carbon and energy fluxes between the surface and the atmosphere at hourly time scale. Most LSMs consist of 1-D column models describing the non-saturated soil (mainly the root-zone), the vegetation and the surface/atmosphere interaction processes. The LSM complexity mainly differs in 1) the number of sources involved in the surface energy balance, 2) the representation of water and thermal soil transfers, 3) the representation of stomatal conductance (see reviews in Olioso et al., 1999; Arora, 2002; Pitman, 2003; Overgaard et al., 2006; Bonan, 2010). For example, the original version of the Interactions between Soil, Biosphere, and Atmosphere (ISBA, Noilhan and Planton (1989)) computes a single energy budget assuming an unique "big leaf" layer. It is a simple bucket model based on the force-restore method with two or three soil layers. The stomatal conductance is simply represented by the Jarvis, (1976) empirical formulation. More advanced LSMs resolve a double-source energy budget (e.g. Sellers et al., 1987) and implement a multi-layer soil diffusion scheme (e.g. Braud et al, 1995b). They can also explicitly simulate photosynthesis (Olioso et al., 1996) and its functional coupling with plant transpiration and they represent vegetation dynamic (Calvet et al., 2008; Egea et al., 2011). Progress in LSMs led to more accurate estimations of energy and water fluxes. This resulted in more realistic simulations of air temperature and humidity of the surface boundary layer in atmospheric models (Noilhan et al., 2011). The improvement of the surface water budget in hydrological models permitted more accurate streamflow forescast (Habets et al., 2008) and drought monitoring (Vidal et al., 2010b). LSMs also proved their usefulness for agronomy application such as irrigation monitoring (Olioso et al., 2005).

This work focuses on the evaluation of the evapotranspiration (ET) simulated from a land surface model over a crop site for a long period of time. ET has been recognized as one of the most uncertain term in the surface water balance (Dolman and de Jeu, 2010; Mueller and Seneviratne, 2014). Uncertainties in simulated ET may propagate large errors in both LSM-atmosphere and LSM-hydrological coupled models. ET uncertainties can arise from (1) errors in the large-scale datasets used to force LSMs, (2) shortcomings in the model structure and (3) errors in the parameter values. Since LSMs were originally designed to be coupled with

atmospheric or hydrological models over large areas, their parametrization is generally parsimonious and their spatial integration is generally based on coarse resolution (~1-10km) maps of parameters. Surface parameters drive a large part of LSM uncertainties and explain most discrepancies between models (Chen et al., 1997; Gupta et al., 1999; Olioso et al., 2002; Boone et al., 2004). The representation of cropland and their temporal dynamic ~~over long period of time~~ need to be improved in LSMs (Lafont et al., 2011; Bonan and Santanello, 2013). Past evaluation studies focused on particular crop types for limited periods of time. They disregarded the succession of crop and inter-crop periods and its impact on the simulated water balance over a long period of time.

The uncertainties in soil hydraulic properties can be large due to significant spatiotemporal variability (Braud et al., 1995a), uncertainties in the estimation method (Baroni et al., 2010; Steenpass et al., 2011) and scale mismatch between the local measurements and the operational scale of the model (Mertens et al., 2005). Errors in soil hydraulic properties can have significant impact on LSM simulations of ET and soil water content (Jacquemin et al., 1990; Braud et al., 1995a; Cresswell and Paydar, 2000). Their impact on the model can be larger than the structural model uncertainties (Workmann and Skaggs, 1994; Baroni et al., 2010). Since the soil hydraulic properties are rarely known over large areas, they are generally derived from empirical pedotransfer functions (PTF) which relate the soil hydrodynamic properties to readily available variables such as soil texture and bulk density (Cosby et al.,1984; Vereecken et al., 1989; Schaap et al., 2000). These functions may not be accurate enough to describe the spatial variability of the soil hydrodynamic characteristics across soil types and their impact on LSM simulations need to be assessed locally (Espino et al., 1996; Baroni et al., 2010).

In this study, the ISBA-A-gs version (Calvet et al., 1998) of the ISBA LSM (Noilhan and Planton, 1989) is considered. ISBA-A-gs includes a coupled stomatal conductance-photosynthesis scheme. Local site studies demonstrated that ISBA (Noilhan and Mahfouf, 1996) and ISBA-A-gs (Gibelin et al., 2008) are able to correctly simulate the diurnal and seasonal time course of energy fluxes and soil water content, over contrasted soil and vegetation types. More variable performances were obtained by Olioso et al., (2002) over wheat fields with possible underestimation of ET.

This paper focuses on the evaluation of the ISBA-A-gs simulations of ET over a 12-year Mediterranean crop succession. We focus on key drivers of simulated ET:

- the soil moisture at saturation which is involved in the simulation of soil evaporation,
- the soil moisture at field capacity, the soil moisture at wilting point and the rooting depth. They define the maximum water stock available for the crop which controls the plant transpiration.

The simulations are assessed over the Avignon 'Remote Sensing and Fluxes' crop site where 14 arable crop cycles and 14 inter-crop periods were monitored through continuous measurements of soil water content and surface fluxes. We represent the succession of crop cycles and inter-crop bare soil periods in the simulations and we assess its impact on the dynamic of simulated and measured evapotranspiration over 12 years. The objectives of this paper consist in:

1. Assessing the performances of the model in its standard implementation which relies on the use of the ECOCLIMAP-II dataset for the surface parameters (Faroux et al., 2013) and the ISBA pedotransfer functions for the soil properties (Noilhan and Laccarère, 1995). No local calibration of the parameters has been done to test the portability of the model parameters over a typical Mediterranean crop site.
2. Assessing the impact of errors in soil parameters on ET simulated over 12 years. We compare the simulations achieved with the soil parameter values derived from the ISBA pedotransfer functions with those achieved with *in situ* values.
3. Selecting the estimates of the soil parameters that lead to the most accurate representation of ET dynamic over the crop succession at the field scale. We test various in situ estimates of the soil parameters derived from laboratory and field measurements. Constant values in time of soil parameters are generally used in LSM while they can vary with crop and climate conditions. We test the use of crop-varying values of wilting point and rooting depth over the crop succession.
4. Evaluating the impact of uncertainties in soil parameters on ET simulations. We question the representativeness of field average estimates of the soil parameters which can be temporally and spatially variable. We compare the ET uncertainties triggered by the soil parameters with those triggered by key vegetation parameter using Monte-

Carlo analyses. Finally, we discuss unresolved scattering between simulations and measurements with respect to modeling and measurement uncertainties.

# 2. Site and measurements

## 2.1 Site characteristics

The "Remote sensing and flux site" of INRA Avignon[1] (France, 4.8789 E, 43.9167N; alt=32m a.s.l) is characterized by a Mediterranean climate with a mean annual temperature of 14°C and a mean annual precipitation of 687 mm. Rainfall mainly occur in autumn (43% of yearly rainfall). It is a flat agricultural field oriented north-south in the prevailing wind direction. The 12-year crop succession studied in this work (Fig. 1 and Table 2) consists in a succession of winter arable crops (wheat, peas) and summer arable crops (sorghum, maize, sunflower). Periods between two consecutive crop cycles lasted ~1-1.5 month in the case of a summer crop followed by a winter crop and ~9-10 months in the reverse case. During inter-crop periods, the soil is mostly bare. Limited wheat regrowths occurred over short periods of time. Irrigation is triggered only for summer crops (every two years) and concerns the May-July period.

## 2.2 Field measurements

***Soil measurements***

Neutron probe was used to retrieve volumetric soil moisture over a 0–1.90 m soil profile with a vertical resolution of 10 cm. To implement the measurements, 3 to 6 neutron probe access tubes were installed at the centre of the field along a north-south transect. A calibration was done for every access tube and soil layer by relating neutron count rates to soil moisture measured by gravimetric method. The average soil moistures at given depth were then used. The measurements were performed on a weekly basis. Surface ground heat flux (G) was derived from 4 heat flux plate measurements located at 5 cm depth and heat storage estimates within the 5 cm layer.

***Plant measurements***

Crop characteristics (leaf area index (LAI), height, biomass) were regularly measured at selected phenological stages. Vegetation height was linearly interpolated on a daily basis.

1 https://www4.paca.inra.fr/emmah_eng/Facilities/In-situ-facilities/Remote-Sensing-Fluxes

Daily interpolation of LAI was achieved using a functional relationship between LAI and the sum of degree-days (Duveiller et al., 2011).

***Micrometeorological measurements***

Half-hourly observations of precipitation, air temperature and humidity, wind speed, atmospheric pressure, radiations, energy fluxes, were continuously performed over the 12-year period. Net radiation (RN) was computed from the measured shortwave and longwave upwelling and downwelling radiations.

Sensible (H) and latent (LE) heat fluxes were computed from an eddy-covariance system. The latter was composed of a 3D sonic anemometer set up in 2001 and of an open-path gas ($H_2O$, $CO_2$) analyzer set up in November 2003. The system was monitored following the state of the art guidelines for cropland sites (Rebmann et al., 2012; Moureaux et al., 2012). Fluxes were computed on 30-min intervals using the EDIRE software[2]. The flux data processing included spike detection on raw data and standard eddy-covariance corrections (coordinate rotation, density fluctuations, frequency-loss). The ECPP[3] software (Beziat et al., 2009) was used to discard spurious flux (e.g. friction velocity and footprint controls) and to apply the Foken et al., (2004) quality control tests on the temporal stationarity and the development of turbulence conditions. In this work, only the best quality class of data (Mauder et al., 2013) was used. An additional threshold of 100 $W.m^{-2}$ on the energy balance non-closure was applied to eradicate very inconsistent fluxes. Direct eddy-covariance measurements of LE are used over the 20 November 2003-18 December 2012 period. They represent 60% of the period (71% if we consider only daytime). When no direct measurement of LE was available (2001-2003 period), LE was estimated as the residue of the energy balance (LE=RN-G-H). Valid direct and indirect LE measurements represent 65% of the 25 April 2001 -18 December 2012 period (77% of daytime). Cumulative ET in mm over given period of time was computed from LE half-hourly measurements.

## 2.3 Soil properties

Table 3 presents the values of the soil parameters averaged over the 0-1.2m soil layer, where most of the root-zone processes occur. The soil moisture at saturation ($\theta_s$) was derived from

2 Robert Clement, © 1999, University of Edinburgh, UK
http://www.geos.ed.ac.uk/abs/research/micromet/EdiRe

3 Eddy Covariance Post Processing, Pierre Béziat, CESBIO, Toulouse, France

soil bulk density measurements performed within the 0-1.2 m layer at different field locations and times over the 12-year period. We used the average value of $\theta_s$ to be representative of the soil structure at the field scale at which the simulations were conducted. The soil moisture at field capacity ($\theta_{fc}$) and wilting point ($\theta_{wp}$) were estimated using the two following methods:

(1) The first method consisted in adjusting a Brooks and Corey (1964) retention curve model over soil matric potential (h) and soil water content measured in laboratory. These measurements were obtained from the Richard pressure plate apparatus at matric potentials of −1, −2, −3, −5, −10, −30, −50, −100, and −150 m (Bruckler et al., 2004). They were collected for 3 soil layers at depths of 0-0.4 m, 0.4-0.8 m and 0.8-1.2 m. A retention model was adjusted for each soil layer and was used to retrieve $\theta_{fc}$ and $\theta_{wp}$ for each soil layer. $\theta_{wp}$ was computed for h=-150 m. Most studies agree on this definition (Boone et al., 1999; Olioso et al., 2002). For $w_{fc}$ two definitions were used. We estimated $\theta_{fc}$ at h=-3.3m which corresponds to the agronomic definition (Olioso et al., 2002) and for an hydraulic conductivity of K= 0.1 mm $d^{-1}$ which can be found in hydrological applications (Wetzel and Chang, 1987; Bonne et al, 1999). $\theta_{wp}$ and $\theta_{fc}$ estimates were averaged over the 0-1.2 m soil profile and their values are reported in Table 3.

(2) In the second method, $\theta_{fc}$ and $\theta_{wp}$ were inferred from field measurements of soil moisture. The time evolution of the root-zone (0-1.2m) soil moisture was analyzed over each crop cycle. Under Mediterranean climate, the root-zone soil moisture generally starts from a upper-level which approximates $\theta_{fc}$. It generally reaches a lower-level at the end of the growing season which often approaches $\theta_{wp}$. The typical evolution of the root-zone soil moisture over the growing season is illustrated in Fig. 3b for wheat. To be consistent with the previous method, we integrated the soil moisture measurements over the 0-0.4 m, 0.4-0.8 m and 0.8-1.2 m soil layers. $\theta_{fc}$ and $\theta_{wp}$ were estimated for each soil layer as the maximum and the minimum, respectively, soil moisture over the growing season. $\theta_{fc}$ and $\theta_{wp}$ values were averaged over the 0-1.2m soil profile for each crop cycle (Table 4). $\theta_{wp}$ vary from one crop to another, but its mean value is close to the one derived from the retention curve. $\theta_{fc}$ shows lower temporal variability but its mean value significantly differs from the retention curve estimate.

The rooting depth ($Z_{root-zone}$) was estimated from the analysis of the evolution in time of the vertical profiles of soil moisture field measurements over the growing season of each crop period. $Z_{root-zone}$ was approximated by the depth at which the soil moisture change in time vanished (Table 4). We assumed that at a given depth, the time variations in soil moisture due to the vertical diffusion and gravitational drainage were smaller than those generated by the plant water uptake (Olioso, et al 2002). This is a reasonable hypothesis for low hydraulic conductivity soil as the one under study.

## 3. The ISBA-A-gs model

### 3.1 Model description

The ISBA model (Noilhan and Planton, 1989; Noilhan and Mahfouf, 1996) is developed at the CNRM/Météo France within the SURFEX surface modeling platform (Masson et al, 2013). In this study, we used the version 6.1 of SURFEX. ISBA relies on a single surface energy budget of a soil-vegetation composite. The surface temperature is simulated using the Bhumralkar (1975) and Blackadar (1976) force restore scheme for heat transfers. An horizontal soil/snow/ice/vegetation surface partitioning is used to simulate the evapotranspiration. The soil water transfers are simulated using a force-restore scheme adapted from Deardoff, (1977) with three reservoirs: the superficial layer of thickness $d_{surf}$=0.01 m designed to regulate the soil evaporation, the root-zone which extends from the surface to the depth $Z_{root-zone}$ and the deep reservoir which extends from the base of the root-zone to the total soil depth. The force restore coefficients were parameterized as a function of the soil hydrodynamic properties which were derived from the Brooks and Corey, (1966) retention model. $\theta_{fc}$ and $\theta_{wp}$ are defined for K=0.1mm $d^{-1}$ and for h=-150m, respectively. The soil parameters are derived from clay and sand fractions using the ISBA pedotransfer functions. The latter were built upon on the Clapp and Hornberger (1978) soil texture classification using statistical multiple regressions (Noilhan and Laccarère, 1995). The force-restore equations and coefficient formulas are given in Boone et al., 1999. Regarding the vegetation processes, we used the A-gs version of ISBA (Calvet et al., 1998; Calvet et al., 2008). A-gs uses a $CO_2$ responsive parameterization of photosynthesis based on the model of Goudriaan et al. (1985) modified by Jacobs et al. (1996). It computes the stomatal conductance as a function of the net assimilation of $CO_2$. It relies on a few number of

physiological parameters which include the $CO_2$ mesophyll conductance (gm). The simulation of the plant response to water stress (Calvet et al., 2000; Calvet et al., 2012) is mainly driven by the maximum root-zone water stock available for the plant (MaxAWC) which is defined by:

$$MaxAWC=Z_{root\text{-}zone}(\theta_{fc}-\theta_{wp}) \quad (1)$$

~~In this work, the model does not simulate the vegetation dynamic and is forced by *in situ* LAI and vegetation height.~~ The model is parametrized through 12 generic land surface patches using the ECOCLIMAP-II database which provides the ISBA surface parameters for ~273 distinct land cover types over Europe (Faroux et al., 2013).

### 3.2 Model implementation at the Avignon site

The simulations were conducted at the field scale. ISBA-A-gs was run at a 5 min time step and 30 min outputs of the state variables were analyzed. Continuous simulations were performed from 25 April 2001 up to 18 December 2012. The 12-year period was split into sub-simulations corresponding to crop and inter-crop periods (Fig. 1). The simulation was initialized once on 25 April 2001 using *in situ* soil temperature and soil moisture measurements for each soil layer. To ensure the continuity between 2 contiguous sub-simulations, each sub-simulation was initialized using the simulated soil moisture and soil temperature of the last time step of the previous sub-simulation. The C3 crop patch was used to represent wheat, pea and sunflower. The C4 crop patch was used for maize and sorghum. Inter-crop periods were represented by the bare soil patch. For crop periods, $Z_{root\text{-}zone}$ represents the depth of the root-zone. For inter-crop period when the soil is bare, it represents the main soil water reservoir. ISBA-A-gs was driven by local meteorological observations. It was forced by *in situ* LAI and vegetation height measurements averaged over 10 days. Crop irrigation was not simulated by the model and the actual amount of irrigation water was added to the local rainfall. The simulations were designed to be representative of the field scale. The in situ soil and vegetation parameters used in the simulations correspond to field average.

## 4 Methodology

This paper focuses on the evaluation of the ISBA-A-gs simulations of ET over the 12-year crop succession of the Avignon site. We focus on key soil parameters for the simulation of ET:

- $\theta_s$ which is involved in the simulation of soil evaporation,
- $Z_{root-zone}$ , $\theta_s$, $\theta_{fc}$ and $\theta_{wp}$ which control the plant transpiration through MaxAWC (Eq. (1)).

Distinct simulations are performed and compared (Table 5) to test the influence of these soil parameters on simulated ET.

## 4.1 Simulation cases

The simulation Sa corresponds to the standard implementation of the model. The vegetation parameters, the rooting depth ($Z_{root-zone}$) and the deep reservoir depth are provided by the ECOCLIMAP-II database (Gibelin et al., 2006; Faroux et al., 2013). ECOCLIMAP-II gives a $Z_{root-zone}$ of 1.5 m which is equal to the average of $Z_{root-zone}$ estimated from the field measurements of soil moisture over each crop cycle (Table 4). The size of the deep reservoir is 0.5 m. Similar soil depths are used for crop and inter-crop periods. The soil hydraulic properties ($\theta_s$, $\theta_{fc}$ , $\theta_{wp}$) are derived from the local soil texture using the ISBA pedotransfer functions (Noilhan and Laccarère, 1995).

The simulations Sb, Sc, Sd and Se use in situ values of $Z_{root-zone}$ , $\theta_s$, $\theta_{fc}$ and $\theta_{wp}$ . The rest of parameters are those used in Sa. Sb, Sc, Sd and Se use the same field-average estimate of $\theta_s$ derived from soil bulk density measurements. They differ only in the in situ values used for $\theta_{fc}$ , $\theta_{wp}$ and $Z_{root-zone}$ (Table 5):

- Sb uses $\theta_{fc}$ and $\theta_{wp}$ derived from the retention curve model established from laboratory measurements. $\theta_{fc}$ corresponds to the matric potential h=-3.3m. $Z_{root-zone}$ is the average of the rooting depths estimated from the soil moisture field measurements over each crop cycle (Table 4).
- Sc uses the same parameters as Sb except that $\theta_{fc}$ corresponds to the hydraulic conductivity K=0.1 mm $d^{-1}$.
- Sd and Se use $\theta_{fc}$ , $\theta_{wp}$ and $Z_{root-zone}$ estimated from the field measurements of soil moisture over each crop cycle (Table 4).
  - Sd uses constant values in time of $\theta_{fc}$ , $\theta_{wp}$ and $Z_{root-zone}$ . It uses the average values computed over the 12-yr crop succession. For the inter-crop periods, $Z_{root-zone}$ is unchanged.

- Se also uses the average value for $\theta_{fc}$ which is lowly variable over the crop succession. For $\theta_{wp}$ and $Z_{root\text{-}zone}$ , it uses the values estimated for each crop cycle. For the inter-crop periods, $Z_{root\text{-}zone}$ is reduced to 0.5 m.

## 4.2 Experiment analyses

We conduct four analyses to address each objective of the paper:

*The first analysis* consists in assessing the performances of the simulation Sa achieved with the standard vegetation and soil parameters over the 12-year crop succession. The impact of the crop succession on the dynamic of simulated ET and its soil/vegetation partitioning are investigated.

*The second analysis* aims at evaluating the impact of errors in the soil parameters on simulated ET. We compare the simulation Sa achieved with the pedotransfer estimates of the soil parameters with Sd performed with the in situ values. We assess :

- the impact of $\theta_{wp}$ over crop periods,
- the role of $\theta_s$ over bare soil periods.

*The third analysis* consists in testing various in situ estimates of the soil parameters and selecting the estimates that lead to the best representation of ET over the crop succession at the field scale. We test:

- The impact of the variability in $\theta_{fc}$ induced by the estimation method comparing Sb, Sc and Sd.
- The impact of using crop-varying values of $\theta_{wp}$ and $Z_{root\text{-}zone}$ comparing Sd which uses constant values in time and Se which uses crop-varying values.
- The impact of reducing the soil reservoir depth on the soil evaporation is tested over the inter-crop periods comparing Sd which uses a soil reservoir depth of 1.5 m and Se for which it is reduced to 0.5 m.

*The last analysis* consists in evaluating the impact of uncertainties in in situ soil parameters on ET simulations. We question the representativeness of field average estimates of the soil parameters which can be temporally and spatially variable. We investigate:

- How the uncertainties in the soil parameters translate into uncertainties in simulated ET ?
- How the uncertainties triggered by the soil parameters compare with those generated by the mesophyll conductance which is a key vegetation parameter involved in the simulation of the stomatal conductance (Calvet et al., 2012) ?

To addres these issues, we conducted two Monte-carlo analyses to generate two ensembles of 100 ET simulations for the Sd simulation case.

- The Monte-Carlo scheme was first applied to the soil parameters tested in this work ($Z_{root-zone}$ , $\theta_s$, $\theta_{fc}$ and $\theta_{wp}$). We considered the uncertainties related to their spatiotemporal variably at the field scale (Table 3 and 4) that we represented by a Gaussian probability distribution function (Table 9).
- The Monte-Carlo was then applied to the mesophyll conductance ($g_m$) which is a key vegetation parameter of the stomatal conductance (Calvet et al., 2012). We assumed a Gaussian probability distribution function for $g_m$ (Table 9). The mean is the standard value (Gibelin et al., 2006) and the standard deviation is derived from literature meta-analysis (Calvet et al., 2000; Calvet et al., 2004).

## 4.3 Simulation performance metrics

The simulations were qualitatively evaluated comparing measured and simulated ET cumulated over the 25 April 2001 -18 December 2012 period. Cumulative ET were concomitantly analyzed with the root-zone soil moisture ($\theta_{root-zone}$) changes in time over selected crop cycles or inter-crop periods to identify the deficiencies in ET modeling. Cumulative values were computed over the time steps for which valid ET measurements were available. Daily daytime ET ($ET_d$) were computed when 90% of daytime measurements were valid for each day.

The simulation performance scores were quantified using the Root Mean Square Error (RMSE), the bias (BIAS), the standard deviation of the differences between simulations and measurements (SDD) and the correlation coefficient (r). These metrics were applied to half-

hourly energy fluxes, $\theta_{root\text{-}zone}$ and $ET_d$. They were computed over the 20 November 2003-18 December 2012 period using only direct eddy-covariance measurements of LE.

# 5 Results

## 5.1 Evaluation of the standard simulation over the 12-year crop succession

***Impact of crop succession on evapotranspiration and soil water content***

Figure 2 illustrates the influence of the succession of crop periods and bare soil inter-crop periods on the temporal evolution of simulated and measured ET and root-zone soil moisture ($\theta_{root\text{-}zone}$).

The early stages of crop periods show high $\theta_{root\text{-}zone}$ which results from rainfall for winter crops and irrigation in May-June for summer crops. Crop growing periods are marked by abrupt increases in ET which is related to plant transpiration. This is concomitant with the depletion of $\theta_{root\text{-}zone}$ which usually reaches its lower level at the end of the crop cycles. Daily ET reaches its highest values at maximum LAI.

Inter-crop periods which follow winter crop cycles are characterized by a dry period in July-August. The low soil water content directly results from the crop water uptake during the previous crop cycle. The soil moisture reaches its upper level in fall which comprises 43% of yearly rainfall. During inter-crop periods, the cumulative rate of ET is low. It is mostly influenced by soil evaporation. Daily ET generally keeps values lower than 1.5 mm $d^{-1}$ . Larger values can be obtained after heavy rain events.

This experiment shows that simulated soil evaporation represents 64 % of cumulative ET over 12 years. It comprises more than 50 % and 95 % of daily ET for 80 % and 60 % of the days, respectively. While plant transpiration may generate significant daily ET during crop growing periods, it concerns only short-time periods compared to soil evaporation.

***Evaluation of energy fluxes***

Table 6 shows the overall performances of simulated energy fluxes. RN is properly simulated (r=0.99) with a low RMSE of 28 W $m^{-2}$. The latter probably falls within the range of the expected measurement errors. H and LE show substantial RMSE (56 W $m^{-2}$ for H and 52 W.$m^{-}$

$^{2}$ for LE). LE has a negative bias of -12 W m$^{-2}$. H shows larger positive bias of 18 W m$^{-2}$. G is markedly overestimated during daytime (daytime bias of 28 W m$^{-2}$).

***Evaluation of simulated evapotranspiration***

Figure 2 shows large underestimation in ET simulated using the ISBA standard vegetation and soil parameters (simulation Sa). The deficit in cumulative ET computed over 65% of the 12-year period amounts to 1490 mm (24% of the measured cumulative ET). The overall bias in daily ET is -0.24 mm d$^{-1}$. This results in an overestimation of the root-zone soil water content which has an overall positive bias of 0.024 m$^{3}$ m$^{-3}$ .

Table 7 provides the performance scores for crop and inter-crop periods. The bias and RMSE are lower for inter-crop periods due to lower flux magnitude. The correlations for daily ET are 0.8 and 0.6 for crop and inter-crop periods, respectively.

For crop cycles, ET and $\theta_{root\text{-}zone}$ are generally properly simulated during the early growing period. ET underestimation occurs during the water stress periods at the end of the crop cycles. The simulated ET shows an early decrease compared to the measured ET. The resulting $\theta_{root\text{-}zone}$ is overestimated at the end of most crop cycles.

For inter-crop periods, ET is mainly underestimated over wet bare soils. Over dry soils, the magnitude of soil evaporation is low and falls within the range of measurement errors. The overestimation of $\theta_{root\text{-}zone}$ at the end of most crop cycles can propagate through the subsequent inter-crop period as illustrated in 2004 and 2006 in Fig. 2. The induced bias in $\theta_{root\text{-}zone}$ persists during the dry period and is generally removed at the rainy period.

## 5.2 Impact of errors in the soil hydraulic properties

***Impact of soil moisture at wilting point***

Figure 3 shows the underestimation of ET and the concomitant overestimation of $\theta_{root\text{-}zone}$ at the end of the crop cycle for the simulation Sa achieved with the pedotransfer estimate of $\theta_{wp}$ . The use of the lower *in situ* $\theta_{wp}$ in Sd leads to higher cumulative ET and greater depletion in $\theta_{root\text{-}zone}$ which are both in better agreement with measurements. No effects are observed for irrigated crops (e.g. maize in Fig. 4).~~The ET underestimation in Sa is related to the overestimation of the pedotransfer estimate of $\theta_{wp}$. The resulting water stock available for the crop's growth (MaxAWC, Eq. (1)) is underestimated which triggers an early water stress in~~

~~the model and an early drop-off of the simulated plant transpiration. This effect is not observed for the irrigated crops (e.g. maize in Fig. 4) and the rainy crop cycles. In these cases, MaxAWC is larger than the crop water needs over the cycle. $\theta_{wp}$ is not reached and no water stress occurs.~~

***Impact of soil moisture at saturation***

Figure 5 shows the underestimation of soil evaporation over wet bare soil for Sa achieved with the pedotransfer estimate of $\theta_s$. For Sd, which was achieved with a lower *in situ* $\theta_s$ , the soil evaporation is increased and the decrease in $\theta_{root\text{-}zone}$ is steeper than for Sa (day 255 to 295 in Fig. 5). This in better agreement with the measurements. The improvement of the simulated soil evaporation is also illustrated at the start of the Maize crop cycle in Fig. 4. ~~The underestimation of the soil evaporation is related to the overestimation of the pedotransfer estimate of $\theta_{sat}$. In the model, the soil evaporation depletes as the superficial (1 cm soil layer) soil moisture drops below $\theta_{fc}$. The temporal dynamic of the superficial soil moisture is mainly driven by the coefficient $C_4$ which is an inverse function of the hydraulic diffusivity and controls the moisture exchange between the superficial layer and the atmosphere (Noilhan and Planton, 1989). The use of the lower *in situ* $\theta_s$ in Sd decreases $C_4$ which tends to maintain higher superficial soil layer and thus higher soil evaporation (Eq. (B4) in Appendix B).~~

## 5.3 Test and selection of in situ soil parameters

***Impact of the variability in estimates of the soil moisture at field capacity***

Impact of $\theta_{fc}$ on simulated soil evaporation is assessed by comparing Sc, Sd and Sb which have increasing $\theta_{fc}$ values. Figure 5a shows that the soil evaporation increases with increasing $\theta_{fc}$. ~~$\theta_{root\text{-}zone}$ tends to converge to the field capacity during the rainy periods (Fig. 5b). The differences in soil evaporation are related to differences in the simulated capillary rises which increase with $\theta_{root\text{-}zone}$ (see Eq. B5 in Appendix B).~~

The high $\theta_{fc}$ value estimated from the laboratory retention curve at h=-3.3m and used in Sb leads to the overestimation of the soil evaporation (Fig. 5a). The performances of ET and $\theta_{root\text{-}zone}$ simulations over inter-crop periods are decreased compared to Sa (Table 7).

The low $\theta_{fc}$ value estimated from the laboratory retention curve at K=0.1mm day$^{-1}$and used in Sc leads to the underestimation of simulated ET (Fig. 5a and Table 7). ~~The gain in superficial~~

~~soil moisture triggered by the use of the *in situ* $\theta_s$ is partly canceled out by the reduction in the simulated capillary rises. The resulting soil evaporation keeps values close to the Sa ones (Fig. 5a). The low $\theta_{fc}$ used in Se triggers larger gravitational drainage than other simulations. This compensates for part of the ET underestimation and explains the reduced bias in simulated $\theta_{root\text{-}zone}$ obtained for Se over the inter-crop periods (Table 7).~~

The use of $\theta_{fc}$ estimated from the soil moisture measurements in Sd leads to better agreement between simulated and measured soil evaporation (Fig. 5a and Table 7) .

~~$\theta_{fc}$ has also an impact on the transpiration through MaxAWC (Eq. (1)). The low $\theta_{fc}$ of Se leads to insufficient MaxAWC and undertesimation of ET over most crop periods (Table 7).~~

***Impact of crop-varying rooting depth and wilting point***

Se, where $Z_{root\text{-}zone}$ and $\theta_{wp}$ were estimated from the soil moisture measurements for each crop cycle, is compared to Sd where mean $Z_{root\text{-}zone}$ and $\theta_{wp}$ estimates are used over the crop succession. Sd and Se show similar cumulative ET over 12 years and close simulation performances (Table 7). The use of $Z_{root\text{-}zone}$ estimated for each crop cycle can locally improve the simulation of ET. This concerns Sorghum, Sunflower or dry wheat cycles (see Se in Fig. 3a) for which the actual rooting depth is greater than the 1.5 m mean value (Table 4). The use of $\theta_{wp}$ estimated for each crop cycle has little impact. This is related to the low $\theta_{wp}$ variability over the crop succession (Table 4).

***Impact of reduced soil reservoir during inter-crop bare soil periods***

For the inter-crop periods, the soil reservoir corresponding to the root-zone keeps the mean value of 1.5m in Sd while it is reduced to 0.5m in Se. The reduction in the soil reservoir over bare soil slightly improves the performances of ET and $\theta_{root\text{-}zone}$ simulations (Table 7). The shallower soil reservoir increases the amplitude of the variations in time of $\theta_{root\text{-}zone}$ (Fig. 5b). ~~This can impact the simulation of soil evaporation through an increase or a decrease of the simulated capillary rises.~~

***Selection of the best simulation over the crop succession***

The simulations Sd and Se achieved with the soil parameters derived from the field soil moisture measurements show substantial reductions in biases in LE, daily ET and $\theta_{root\text{-}zone}$ compared to the standard simulation Sa (Table 7). Sd achieved with the average values of the

soil parameters shows the lowest biases in ET. The deficit in cumulative ET over 12-yr which amounts to 24% for Sa is reduced to 6.7 % for Sd. It is 22% for Sa and 0.45% for Sd if only direct measurements of LE are used over the 2004-2012 period. Figure 6 shows that Sd properly reproduces the time evolution of measurements over the crop succession.

The RMSE for LE and daily ET are not reduced in Sd compared to Sa. They mostly represent random differences between measurements and simulations. For Sd, the standard deviation of these random differences amounts to 53 W $m^{-2}$

### 5.4 Impact of uncertainties in situ soil parameters

We represent the uncertainties in simulated ET using cumulative values over the 2004-2012 period for which direct ET measurements are available. We display the simulation Sd, the ensemble of the Monte-Carlo simulations and the 95% percentile interval of simulated ET. The percentiles are computed over the empirical distribution of cumulative ET values. Fig 6 shows:

- The spatiotemporal variability of the soil parameters can generate large uncertainties in ET. The 95% percentile interval represents 867 mm (23%) of cumulative ET over 12 years.
- The uncertainties in the mesophyll conductance have a lower impact. The 95% percentile interval represents 83 mm ( 2%) of cumulative ET over 12 years.

## 6 Discussion

We tested 3 types of soil parameter estimates derived from:

- the ISBA pedotransfer functions,
- the retention curve model adjusted over laboratory measurements,
- the analysis of field measurements of soil moisture vertical profiles.

In the following section, we discuss the uncertainties in each type of soil parameter estimate and we analyse their impact on simulated ET. In the two last sections, we discuss other sources of modelling and measurement uncertainties.

## 6.1 Uncertainties in the soil parameters

### 6.1.1 Errors in the pedotransfer estimates

Most of ET underestimation reported for the standard implementation of the model (Sa) is due to the overestimation of the wilting point ($\theta_{wp}$) and the soil moisture at saturation ($\theta_s$) by the ISBA pedotransfer functions (Table 5). The use of in situ values derived from soil moisture measurements in Sd substantially reduces the bias in ET (Fig .6). The deficit in simulated ET triggers an increase of the simulated drainage that is probably overestimated. The increase in simulated ET from the simulation Sa to the simulation Sd is 1375 mm over 12 years. The decrease in simulated drainage is 1418 mm.

The overestimation of $\theta_{wp}$ triggers the underestimation of the water stock available for the crop's growth (MaxAWC, Eq. (1)). Early water stress is simulated which conducts to the underestimation of the simulated plant transpiration at the end of the crop cycle. This effect is not observed for irrigated crops (e.g. maize in Fig. 4) and rainy crop cycles. In these cases, the supply of water by irrigation is sufficient to satisfy crop water needs over the growing season. $\theta_{wp}$ is not reached and no water stress occurs.

The overestimation of $\theta_s$ triggers the underestimation of the soil evaporation over wet bare soil. The simulated soil evaporation depletes as the simulated superficial soil moisture drops below field capacity (Eq. A1 and A2, Appendix A). The temporal dynamic of the superficial soil moisture is mainly driven by the coefficient $C_1$ which is an inverse function of the hydraulic diffusivity and controls the moisture exchange between the superficial layer and the atmosphere (Noilhan and Planton, 1989). The overestimation of $\theta_s$ leads to large values of $C_1$ which depletes the superficial soil moisture and conducts to the underestimation of soil evaporation (Eq. (A4) in Appendix A).

Large discrepancies have been reported between pedotransfer functions (PTFs) which are prone to distinct sources of uncertainties (Espino et al., 1996; Baroni et al., 2010; Gijsman et al., 2013). The first shortcoming concerns their representativeness of soil property variability. The ISBA pedotransfer functions were established upon the Clapp and Hornberger (1978) database. These functions were calibrated using mean values of soil properties over few classes of soil texture and do not represent the variability within each soil class. Besides maps of soil texture may not be accurate enough at regional scale. The second source of uncertainty

is related to the estimation method. PTFs were designed to be applied over readily available variables such as soil texture. Improvements of the prediction equations may require the use of additional predictors related to soil structure (Vereecken et al, 1989). Most PTFs are based on simple statistical regressions such as the ISBA ones (Noilhan and Laccarère, 1995). The more advanced ROSETTA PTF (Schaap et al., 2001) addresses the uncertainty in the predicted soil parameters through the use of an ensemble of functions calibrated over distinct soil datasets. Such model provides essential information on the variance and covariance of the hydraulic properties (Scharnagl et al., 2011) which are required to propagate the uncertainties in the LSM simulations.

### 6.1.2 Uncertainties in the laboratory measurements of field capacity

Field capacity ($\theta_{fc}$) mainly impacts the simulation of soil evaporation. It drives the upper level of $\theta_{root\text{-}zone}$ during the wet bare soil period. The differences in soil evaporation simulated with various $\theta_{fc}$ (Fig. 5) are related to differences in simulated capillary rises to the surface which increase with the magnitude of $\theta_{root\text{-}zone}$ (see Eq. A5 in Appendix A). The $\theta_{fc}$ value at h=-3.3m estimated from the adjustment of the retention curve over laboratory measurements is too high to be consistent with the field measurements of soil moisture during wet bare soil periods. It leads to the overestimation of the simulated soil evaporation (Sb). The $\theta_{fc}$ estimate at K=0.1 mm $d^{-1}$ used in Sc is too low and leads to the underestimation of the soil evaporation. This partly compensates for the increase in soil evaporation triggered by the use of in situ $\theta_s$ and explains that the resulting soil evaporation of Sc keeps values close to the Sa ones (Fig. 5a).

Field capacity has also an impact on the transpiration. The low $\theta_{fc}$ used in Sc leads to insufficient MaxAWC that explains the undertesimation of ET over most crop periods (Table 7)

Various studies have questioned the use of hydraulic properties inferred from laboratory techniques to simulate water transfers at the field scale (Basile et al., 2003; Mertens et al., 2005; Scharnagl et al., 2010). Laboratory experiments may not be representative of field conditions. Gravimetric measurements can disturb the actual soil structure. Small soil samples cannot capture the spatial and vertical heterogeneity of the soil structure at the field scale

which can be substantially influenced by macroporosity and soil operations (Mertens et al., 2005). Single measurement cannot resolve the changes in soil structure caused by crop development and tillage operations (Baroni et al., 2010).

### 6.1.3 Soil parameters derived from soil moisture field measurements

The most accurate simulation is achieved with the average values of $Z_{root\text{-}zone}$, $\theta_{fc}$ and $\theta_{wp}$ derived from the analysis of soil moisture measurements over each crop cycle (Sd case). Field measurements of soil moisture better resolve the intra-field spatial variability through 4 neutron probes compared to the laboratory measurements. The analysis in time of the vertical profiles of soil moisture over the growing season provides meaningful estimates of the wilting point, the field capacity and the rooting depth for each crop cycle. Their mean values are accurate enough to represent the crop water needs and accurately simulate ET at the field scale over the 12-year crop succession. The use of crop-varying rooting depth and wilting point and the reduction of the soil reservoir depth over the inter-crop periods have little impact on the overall simulation performances. The use of constant soil depths over the crop succession is preferable to ensure the conservation of mass in the force-restore simulation of the water balance over a long period of time.

However, one can question the representativeness of field average in situ estimates of soil parameters which can be spatially and temporally variable. For example, the soil moisture at saturation is prone to large spatiotemporal variations due to macroporisity and impact of soil operations on the structure of the 0-0.4 m soil layer. We showed in Fig. 6 that the spatiotemporal variability in the soil parameters can generate large uncertainties in simulated ET over 12 years. These uncertainties are much larger than those generated by the mesophyll conductance. They explain part of the unresolved random differences between simulated and measured ET.

## 6.2 Structural model uncertainties

A first shortcoming of the force-restore scheme concerns the lack of description of vertical heterogeneity of soil properties. Attempts to account for soil stratification were achieved through re-scaling functions of the force-restore coefficients (Montaldo and Albertson, 2001; Decharme et al., 2006). The increase in hydraulic conductivity at saturation ($K_{sat}$) generally

observed in the ~0-0.4m soil layer of crop fields can be represented in SURFEX using a decreasing exponential profile of $K_{sat}$ between the surface and the bottom of the root-zone (Decharme et al, 2006). We tested the use of a $K_{sat}$ exponential profile for the case Sd (not shown here). We found that it decreases the performances of LE and daily ET simulations. It increases the hydraulic diffusivity which results in a frequent overestimation of the soil evaporation. A second shortcoming of the force-restore is the lack of root profile. This could particularly affect the representation of the effect of water stress on plant transpiration (Desborough et al., 1997; Braud et al., 2005; Fan et al., 2006). A multi-layer diffusion scheme can explicitly represent the soil vertical heterogeneity and the interactions between plant and soil more accurately (Decharme et al., 2011). However, the performances of such detailed models rely on accurate parametrization of root profile and soil vertical heterogeneity which may not be available at large-scale (Olioso et al., 2002, Demarty et al., 2004). Further works are needed to evaluate whether such model improves the simulation of the water balance over a crop succession.

Substantial differences in simulated soil evaporation between LSMs have been attributed to differences in soil evaporation formulations and representation of the soil resistance to water diffusion (Mahfouf and Noilhan, 1991; Desborough et al., 1996). In ISBA, a bulk aerodynamic formulation is used (Mahfouf and Noilhan, 1991). The potential soil evaporation is weighted by a surface relative humidity coefficient parametrized as a function of the superficial soil moisture (Eq. A2 in Appendix A). This may not be accurate enough to describe the resistance of a drying soil to water vapor diffusion which depends on both soil structure and texture (Kondo et al., 1990; Merlin et al, 2011).

The remaining underestimation in ET during the crop senescence despite the use of the *in situ* soil hydraulic parameters (e.g. Maize in 2001 in Fig. 4b) could be attributed to inaccurate partitioning between soil evaporation and transpiration at low LAI (Olioso et al., 2002). This could be related to unrealistic decrease of the vegetation cover which is a function of LAI in the model while the senescent crop is covering a non negligible soil fraction and has radiative and aerodynamic impacts. The use of a single source energy balance can also impact ET partitioning (Olioso et al., 2002). Other factors related to the parametrization of photosynthesis, canopy conductance and water stress could also cause transpiration underestimation.

## 6.3 Uncertainties in eddy covariance measurements

Random errors in eddy covariance measurements arise from turbulence sampling errors, instrument errors and flux footprint uncertainties (Richardson et al., 2006). We applied the Richardson et al. (2006) method (explained in Appendix B) to compute the standard deviation of the measurement random error for various classes of LE values. Results are given in Table B1. Random errors are very likely to cancel out when measurements are cumulated over long period of time. However, they can explain a large part of the unresolved random differences between the simulations and the measurements at half-hourly and daily time scales.

Eddy-covariance are also prone to systematic errors. Particularly, the eddy-covariance system could fail to resolve low frequency turbulence structures that could lead to the underestimation of eddy fluxes (Foken, 2008). This results in the non closure of the measured energy balance (EB) which is a critical source of uncertainties when these measurements are compared to LSM simulations. Other reasons for the EB non-closure include horizontal and vertical advection, inaccuracies in the eddy covariance processing and footprint mismatch between the eddy fluxes and the other energy fluxes (RN,G) (Foken, 2008; Leuning et al., 2012). The application of an energy imbalance threshold of 100 $W.m^{-2}$ minimized the magnitude of the EB non-closure of our dataset. The mean and the standard deviation of the absolute value of the EB non-closure are 28 $W.m^{-2}$ and 22 $W.m^{-2}$, respectively. This is comparable to the non-closure reported for cropland in Wilson, et al. (2002); Hendricks et al. (2010) and Ingwersen et al. (2010).

The uncertainties in eddy-covariance measurements are further assessed comparing the direct measurement of LE with two other estimates. The first estimate is computed as the residue of the energy balance assuming that H is error-free. The second estimate is derived from the bowen ratio (ratio between H and LE) assuming that the bowen ratio is correctly estimated (Twine et al., 2000). The SD of the differences in LE between the direct measurement and the other estimates fall between 24 and 36 $W\ m^{-2}$ (Table 8). The MD at half-hourly time scale fall between 3 and 7 $W\ m^{-2}$. The MD in cumulative ET over 12 years between the bowen ratio estimate and the direct measurement represents 727 mm (12%). It is 310 mm (5%) between the estimate derived from the residue of the energy balance and the direct measurement. The deficits in simulated ET reported in this work are thus probably larger due to likely underestimation of ET by eddy-covariance measurements.

## 7 Summary

In this study, the SURFEX/ISBA-A-gs simulations of evapotranspiration (ET) are assessed at the field scale over a 12-year Mediterranean crop succession. The model is evaluated in its standard implementation which relies on the use of the ISBA pedotransfer function estimates of the soil properties. The originality of this work consists in explicitly representing the succession of crop cycles and inter-crop bare soil periods in the simulations and assessing its impact on the dynamic of simulated and measured evapotranspiration over a long period of time. The analysis focuses on key soil parameters which drive the simulation of ET, namely the rooting depth, the soil moisture at saturation, the soil moisture at field capacity and the soil moisture at wilting point. The simulations achieved with the standard soil parameters estimated from the ISBA pedotransfer functions are compared to those achieved with the *in situ* values. Various *in situ* estimates of the soil parameters are tested and the estimates that lead to the most accurate representation of ET over the crop succession at the field scale are selected. Finally, the impact of uncertainties in in situ soil parameters on ET simulations is evaluated and compared with the uncertainties triggered by a key vegetation parameter (the mesophyll conductance).

Evapotranspiration mainly results from the soil evaporation when it is simulated over a succession of crop cycles and inter-crop periods for Mediterranean croplands. The crop transpiration generates high ET over short-time periods while the soil evaporation represents more than 50% of ET for 80% of the days. Accounting for crop succession in LSM is thus essential to accurately estimate ET amount and ET temporal dynamic which are both critical to properly represent land-surface atmosphere interactions.

ET simulated with the standard surface and soil parameters of the model is largely underestimated. The deficit in cumulative ET amounts to 24% over 12 years. The bias in daily daytime ET and root-zone soil moisture are -0.24 mm $d^{-1}$and 0.024 $m^3$ $m^{-3}$. ET underestimation is mainly related to the overestimation of the soil parameters by the ISBA pedotransfer functions. The overestimation of the wilting point triggers the underestimation of the water stock available for the crop's growth which conducts to the underestimation of the simulated plant transpiration at the end of the crop cycle. The overestimation of the soil moisture at saturation triggers an underestimation of the water diffusivity in the superficial layer which reduces the soil evaporation during wet periods.

The field capacity value at h=-3.3m derived from laboratory measurements triggers frequent overestimation of the simulated soil evaporation which is related to the lack of representativeness of the soil structure variability at the field scale. The field capacity estimate at K=0.1 mm.day$^{-1}$ is too low and leads to the underestimation of evapotranspiration.

The most accurate simulation is achieved with the average values of the soil parameters derived from the analysis of field measurements of soil moisture vertical profiles over each crop cycle. The use of crop-varying rooting depth and wilting point and the reduction of the soil reservoir depth during the inter-crop periods have little impact on the ET simulation performances over 12 years.

The spatiotemporal variability of the soil parameters generate substantial uncertainties in simulated ET (the 95% confidence interval represents 23% of cumulative ET over 12-years) which are much larger than the uncertainties triggered by the mesophyll conductance.

The measurement random errors tend to cancel out when measurements are cumulated over long period of time. They explain a large part of the unresolved scattering between simulations and measurements at half-hourly time scale. The deficits in simulated ET reported in this work are probably larger due to likely underestimation of ET by eddy-covariance measurements.

Other modeling uncertainties could concern the lack of soil vertical heterogeneity and root profile representation in the force-restore water transfer scheme, inaccurate ET partitioning between the soil and the vegetation at low LAI, inaccurate representation of the soil resistance in the soil evaporation formulation and shortcomings in the representation of vegetation processes (e.g. photosynthesis).

This work highlights the prevailing role of the soil parameters in the simulation of ET dynamic over a multi-year crop succession. Accounting for uncertainties in soil properties is of paramount importance for the spatial integration of land surface models. Methods need to developed to spatially retrieve the soil parameters and their uncertainties at regional scale. We showed that pedotransfer functions can be inaccurate. Field measurements of soil moisture are generally not available at regional scale. Satellite observations of soil moisture and vegetation status can be used to retrieve the soil properties over large areas. Bayesian inverse modelling

(Vrugt et al., 2009) are appropriate methods to calibrate the soil parameters and translate their uncertainties into uncertainties in the simulated fluxes (Mertens et al., 2004; Scharnagl et al , 2011). All sources of modelling errors (forcing data, vegetation and soil parameters, model structure) can be adequately incorporated in the analysis. Our results will serve as a basis for such complementary work to monitor ET and its uncertainties over cropland.

# APPENDICES

## Appendix A : The soil evaporation in the force-restore scheme

The ISBA soil evaporation (E) is given by

$$E=(1-veg)\rho_a C_H V[h_u q_{sat}-q_a] \quad \text{(A1)}$$

where veg is the fraction of vegetation cover, $\rho_a$ is the dry air density, $C_H$ is the drag coefficient, V is the wind speed, $q_{sat}$ is the surface specific humidity at saturation and $q_a$ is the air specific humidity at the reference height. $h_u$ is the air relative humidity at the surface and is computed as :

$$h_u=0.5[1-\cos(min(\frac{\theta_{surf}}{\theta_{fc}},1)\pi)] \quad \text{(A2)}$$

where $\theta_{surf}$ is the superficial soil moisture and $\theta_{fc}$ is the soil moisture at field capacity. E is at its potential rate when $\theta_{surf}>\theta_{fc}$ (hu=1). It depletes as $\theta_{surf}$ drops below $\theta_{fc}$. For $h_u*q_{sat}<q_a$, if $q_{sat}< q_a$ a dew flux is triggered and if $q_{sat}> q_a$ the soil evaporation is set to zero.

The time course of $\theta_{surf}$ is given by the force-restore equation:

$$\frac{\partial\theta_{surf}}{\partial t}=\frac{C_1}{\rho_w d_1}(P-E)-\frac{C_2}{\tau}(\theta_{surf}-\theta_{eq}) \quad \text{(A3)}$$

In Eq. (A3), $\rho_w$ is the liquid water density, P is the flux of water reaching the surface and $\tau$ is the restore constant of one day.

The coefficient $C_1$ is driving the moisture exchange between the surface and the atmosphere. It is an inverse function of the hydraulic diffusivity (Noilhan and Planton, 1989; Eq. A.4).

$$C_1=C_{1,s}d_{surf}(\frac{\theta_s}{\theta_{surf}})^{0.5b+1} \quad \text{(A4)}$$

In Eq. (A4), $C_{1,s}$ is the value at saturation (in $m^{-1}$) calibrated as a function of clay fraction and b is the slope of the Brooks and Corey, 1964 retention curve. $C_1$ is minimum at saturation and increases as the soil surface dries out. It reaches its maximum for $\theta_{surf}=\theta_{wp}$ . For $\theta_{surf}$ lower than $\theta_{wp}$ , water vapor phase transfers are prevailing. $C_1$ is represented by a Gaussian formulation (Giordani et al., 1993; Giard and Bazile, 1996) and decreases with increasing soil temperature and decreasing soil moisture.

The second term in the right-hand side of Eq. (A3) represents the vertical water diffusion between the root-zone and the superficial layer. It is ruled by the diffusion coefficient $C_2$ (Eq. (A5)) which quantifies the rate at which the soil moisture profile between layer 1 and 2 is restored to the equilibrium $\theta_{eq}$ (water content at the balance between the gravity and the capillary forces).

$$C_2 = C_{2ref}\left(\frac{\theta_{root-zone}}{\theta_s - \theta_{root-zone} + \theta_l}\right) \qquad \text{(A5)}$$

In Eq. A5, $\theta_{root\text{-}zone}$ is the root-zone soil moisture, $\theta_1$ is a numerical constant . $C_{2ref}$ is the mean value of $C_2$ for $\theta_2=0.5\ \theta_s$ and is computed as a function of clay fraction. $C_2$ is an increasing function of $\theta_{root\text{-}zone}$.

In ISBA, the force-restore water transfer scheme and the resulting soil evaporation strongly depend on soil texture (Jacquemin et al, 1990). Coarse soil texture are characterized by high soil hydraulic diffusivity and conductivity which are represented in the model by low $C_1$ and high $C_2$, respectively. For sandy soil, low value of $C_1$ reduces the depletion of $\theta_{surf}$ due to soil evaporation and high $C_2$ enhances the supply of $\theta_{surf}$ by capillary rises. The resulting daily variations of $\theta_{surf}$ are low and the values of $\theta_{surf}$ are frequently higher than $\theta_{fc}$. The resulting soil evaporation is frequently at its potential rate. Conversely, clay soils have higher $C_1$ and lower $C_2$. This leads to more rapid depletion of $\theta_{surf}$ which keeps lower values compared to sandy soil. The subsequent soil evaporation drops since it is more rapidly limited by the soil water supply.

## Appendix B: Characterization of the random errors in the eddy covariance measurements

The Richardson et al. (2006) method to assess the random errors in eddy-covariance measurements consists in selecting 24h apart pairs of measurements acquired under equivalent environmental conditions. The latter are defined by differences in vapor pressure deficit within 0.15kPa, wind speed within 1m.s$^{-1}$, air temperature within 3°C and photosynthetic photon flux within 75 µmol.m$^{-2}$.s$^{-1}$. Compared to the original method, additional criteria were implemented: wind direction within +/-15°, footprint within 30%, surface soil moisture within 0.03 m$^3$.m$^{-3}$, incoming solar radiation within 50 W.m$^{-2}$. The measurement pairs ($x_1$ and $x_2$) are assumed to be two measurements of the same flux F at two distinct times.

$$x_1 = F + \delta_1 \quad \text{(B1)}$$

$$x_2 = F + \delta_2 \quad \text{(B2)}$$

δ represents the random error which is assumed to be uncorrelated in time and identically distributed in time. Richardson et al. (2006) showed that the standard deviation of the random error ($\sigma_\delta$) is :

$$\sigma_\delta = \sigma(x_1 - x_2)/\sqrt{2} \quad \text{(B3)}$$

where $\sigma(x_1\text{-}x_2)$ is the standard deviation of the differences between the values of the measurement pairs. In our experiment, we assume that $x_1$ -$x_2$ follows a Gaussian distribution. Table B.1 provides $\sigma_\delta$ computed for distinct classes of LE values.

Table B1: Standard deviation ($\sigma_\delta$) of the random error of the LE measurements computed for distinct classes of LE values. N is the number of measurement pairs used to estimate the random error.

| | Ranges of LE flux ($W.m^{-2}$) | | | | | |
|---|---|---|---|---|---|---|
| | < 0 | [0,50] | [50,100] | [100,200] | >200 | |
| N | 627 | 2592 | 615 | 233 | 117 | |
| $\sigma_\delta$ | 4.8 | 7.8 | 14.9 | 23.4 | 53.4 | |

## References


Arora, V.K.: Modeling vegetation as a dynamic component in soil- vegetation-atmosphere transfer schemes and hydrological models, Rev. Geophys., 40(2), 1006, 2002.

Basile, A., Ciollaro, G., and Coppola, A.: Hysteresis in soil water characteristics as a key to interpreting comparisons of laboratory and field measured hydraulic properties, Water Resour. Res., 39, 1355, doi:10.1029/2003WR002432, 2003.

Baroni, G., Facchi, a., Gandolfi, C., Ortuani, B., Horeschi, D., van Dam, J.C.: Uncertainty in the determination of soil hydraulic parameters and its influence on the performance of two hydrological models of different complexity, Hydrol. Earth Syst. Sci. 14, 251–270, 2010.

Beziat, P., Ceschia, E., Dedieu, G.: Carbon balance of a three crop succession over two cropland sites in South West France, Agr. Forest Meteorol., 149, 1628-1645, 2009.

Bhumralkar, C. M.: Numerical experiments on the computation of ground surface temperature in an atmospheric general circulation model, J. Appl. Meteorol., 14, 1246–1258, 1975

Blackadar, A. K.: Modeling the nocturnal boundary layer. Preprints, Third Symp. on Atmospheric Turbulence, Diffusion and Air Quality, Raleigh, NC, Amer. Meteor. Soc., 46–49, 1976.

Bonan,G.: Land surface processes in climate models. In Ecological Climatology, Ed Bonan, G. Cambridge, 2010.

Bonan, G B., Santanello, J.A.: Modelling the land-atmosphere interface across scales: from atmospheric science to Earth system science, ILEAPS newsletter, 13, 6-8, 2013.

Boone, A., Calvet, J.-C., Noilhan, J.: Inclusion of a Third Soil Layer in a Land Surface Scheme Using the Force–Restore Method, J. Appl. Meteorol., 1611-1630, 1999.

Boone, A. and coauthors: The Rhone-Aggregation Land Surface Scheme Intercomparison Project: An Overview, J. Climate, 187-208, 2004.

Braud I., Dantas-Antonio, A.C., Vauclin,M. : A stochastic approach to studying the influence of the spatial variability of soil hydraulic properties on surface fluxes, temperature and humidity. J. Hydrol., 165, 283-310, 1995a.

Braud, I., Dantas-Antonino, A.C., Vauclin, M., Thony, J-L., Ruelle, P.: A simple soil-plant atmosphere transfer model (SiSPAT) development and field verification, J. Hydrol., 166, 213-250, 1995b.

Braud, I., Varado, N., Olioso, A. : Comparison of root water uptake modules using either the surface energy balance or potential transpiration, J. Hydrol., 301, 267–286, 2005.

Brooks, R. H., and Corey, A.T.: Properties of porous media affecting fluid flow, J. Irrig. Drain. Amer. Soc. Civil Eng., 2, 61–88, 1966.

Bruckler, L., Lafolie, F., Doussan, C., Bussières, F.: Modeling soil-root water transport with non-uniform water supply and heterogeneous root distribution, Plant and Soil, 260, 205-224, 2004.

Calvet, J.-C., Noilhan, J., Roujean, J-L., Bessemoulin, P., Cabelguenne, M., Olioso, A., Wigneron, J-P.: An interactive vegetation SVAT model tested against data from six contrasting sites, Agr. Forest Meteorol., 92, 73-95, 1998.

Calvet, J.-C.: Investigating soil and atmospheric plant water stress using physiological and micrometeorological data. Agr. Forest Meteorol., 103, 229-247, 2000.

Calvet, J.-C., V. Rivalland, C. Picon-Cochard, and Guehl, J.-M. : Modelling forest transpiration and CO 2 fluxes - Response to soil moisture stress, Agric. For. Meteorol., 124, 143 – 156, 2004

Calvet, J.-C., Gibelin, A.-L., Roujean, J.-L., Martin, E., Moigne, P. L., Douville, H., Noilhan, J.: Past and future scenarios of the effect of carbon dioxide on plant growth and transpiration for three vegetation types of southwestern France, Atmospheric Chemistry and Physics, 8, 397-406, 2008.

Calvet, J.-C., Lafont, S., Cloppet, E., Souverain, F., Badeau, V., Le Bas, C.: Use of agricultural statistics to verify the interannual variability in land surface models: a case study over France with ISBA-A-gs, Geoscientific Model Development, 5, 37-54, 2012.

Chen, T. H., and Coauthors: Cabauw experimental results from the project for intercomparison of land-surface parameterization schemes, J. Climate, 10, 1194–1215, 1997.

Clapp, R., Hornberger, G.: Empirical equations for some soil hydraulic properties. Water Resour. Res., 14, 601–604, 1978.

Cosby, B. J., G. M. Hornberger, R. B. Clapp, Ginn, T.R.: A statistical exploration of the relationships of soil moisture characteristics to the physical properties of soils, Water Resour. Res., 20, 682–690, 1984.

Cresswell, H. P. and Paydar, Z.: Functional evaluation of methods for predicting the soil water characteristic, J. Hydrol., 227, 160– 172, 2000.

Deardorff, J. W.: A parameterization of ground surface moisture content for use in atmospheric prediction models, J. Appl. Meteorol., 16, 1182–1185, 1977.

Decharme, B., Douville, H., Boone, A.; Habets, F., Noilhan, J.: Impact of an Exponential Profile of Saturated Hydraulic Conductivity within the ISBA LSM: Simulations over the Rhône Basin, J. Hydrometeorol., 61-80, 2006.

Decharme, B., Boone, a., Delire, C., Noilhan, J.: Local evaluation of the Interaction between Soil Biosphere Atmosphere soil multilayer diffusion scheme using four pedotransfer functions, J. Geophys. Res., 116, D20126, 2011.

Demarty, J., Ottlé, C., Braud, I., Olioso, A., Frangi, J-P., Bastidas, L.A., Gupta, H.: Using a multiobjective approach to retrieve information on surface properties used in a SVAT model, J. Hydrol., 287, 214-236, 2004.

Desborough, C.E., Pitman, A., Irannejad, P.: Analysis of the relationship between bare soil evaporation and soil moisture simulated by 13 land surface schemes for a simple non-vegetated site, Global and Planetary Change 13, 47–56, 1996.

Desborough, C.E.: The Impact of Root Weighting on the Response of Transpiration to Moisture Stress in Land Surface Schemes, Monthly Weather review, 1920–1930, 1997.

Dolman, A.J, De Jeu, R. A. M. : Evaporation in Focus. Nature Geosciences, 3, 296, 2010.

Duveiller, G., Weiss, M., Baret, F., Defourny, P.: Retrieving wheat Green Area Index during the growing season from optical time series measurements based on neural network radiative transfer inversion, Remote Sens. Environ., 115, 887-896, 2011.

Egea, G., Verhoef, A., Vidale, P. L.: Towards an improved and more flexible representation of water stress in coupled photosynthesis-stomatal conductance models. Agr. Forest Meteorol., 151, 1370-1384, 2011.

Espino, A., Mallants, D., Vanclooster, M., Feyen, J.: Cautionarynotes on the use of pedotransfer functions for estimating soil hydraulic properties, Agric. Water Manage., 29, 235– 253, 1996.

Fan, Y., Van den Dool, H. M., Lohmann, D., Mitchell, K.: 1948–98 U.S. hydrological reanalysis by the NOAH land data assimilation system, J. Climate, 19, 1214–1237, 2006.

Faroux, S., Kaptué Tchuenté, A. T., Roujean, J.-L., Masson, V., Martin, E., Le Moigne, P.: ECOCLIMAP-II/Europe: a twofold database of ecosystems and surface parameters at 1 km resolution based on satellite information for use in land surface, meteorological and climate models, Geosci. Model Dev., 6, 563-582, 2013.

Foken, T., Mauder, M., Mahrt, L., Amiro, B., Munger, W.: Post-field data quality control, in: Lee, X., et al. (Eds.), Handbook of Micrometeorology, 181–208, 2004.

Foken, T.: The energy balance closure problem: an overview, Ecological Applications, 18, 1351-1367, 2008.

Giard, D., Bazile, E.: Implementation of a New Assimilation Scheme for Soil and Surface Variables in a Global NWP Model, Monthly Weather Review, 997-1015, 2000.

Gibelin, A.-L., Calvet, J-C., Roujean, J-L., Jarlan, L., Los, S. O.: Ability of the land surface model ISBA-A-gs to simulate leaf area index at the global scale: Comparison with satellites products, J. Geophys. Res., 111, 1-16, 2006.

Gibelin, A.-L., Calvet, J.-C., Viovy, N.: Modelling energy and CO 2 fluxes with an interactive vegetation land surface model-Evaluation at high and middle latitudes, Agr. Forest Meteorol., 148, 1611-1628, 2008.

Giordani, H., Noilhan, J., Lacarrère, P., Bessemoulin, P., Mascart, P.: Modelling the surface processes and the atmospheric boundary layer for semi-arid conditions, Agr. Forest Meteorol., 80, 263-287, 1996.

Gijsman, A. J., Jagtap, S. S., and Jones, J. W.: Wading through a swamp of complete confusion: how to choose a method for estimating soil water retention parameters for crop models, Europ. J. Agronomy, 18, 77–106, 2003.

Goudriaan, J., van Laar, H. H., van Keulen, H., and Louwerse, W.: Photosynthesis, CO 2 and plant production, in: Wheat Growth and Modelling, edited by: Day, W. and Atkin, R. K., NATO ASI Series, Plenum Press, New York, Series A, 86, 107–122, 1985.

Gupta, H. V., Bastidas, L. a., Sorooshian, S., Shuttleworth, W.J., Yang, Z.L.: Parameter estimation of a land surface scheme using multicriteria methods, J. Geophys. Res., 104, 19491, 1999.

Habets, F., Boone, A., Champeaux, J. L., Etchevers, P., Franchisteguy, L., Leblois, E., Ledoux, E., Moigne, P. L., Martin, E., Morel, S., Noilhan, J., and Viennot, P.: The SAFRAN-ISBA-MODCOU hydrometeorological model applied over France, 113, 1-18, 2008.

Hendricks Franssen, H.J., Stöckli, R., Lehner, I., Rotenberg, E., Seneviratne, S.I.: Energy balance closure of eddy-covariance data: A multisite analysis for European FLUXNET stations, Agr. Forest Meteorol., 150, 1553-1567, 2010.

Ingwersen, J., Steffens, K., Högy, P., Zhunusbayeva, D., Poltoradnev, M., Gäbler, R., Wizemann, H., Fangmeier, A., Wulfmeyer, V.; Streck, T.: Comparison of Noah simulations with eddy covariance and soil water measurements at a winter wheat stand, Agr. Forest Meteorol., 151, 345-355, 2011.

Jacquemin, B., and Noilhan, J.: Sensitivity study and validation of a land surface parameterization using the hapex-mobilhy data set, Boundary Layer Meteorology, 52, 93-134, 1990.

Jarvis, P.G.: The interpretation of the variations in water potential and stomatal conductance found in canopies in the field, Philosophical Transactions of the Royal Society, London, Ser. B., 273, 593–610, 1976.

Jacobs, C. M. J., Van den Hurk, B. J. J. M., and De Bruin, H. A. R.: Stomatal behaviour and photosynthetic rate of unstressed grapevines in semi-arid conditions, Agr. Forest Meteorol., 80, 111–134, 1996

Kondo, J., Nobuko, S., Takeshi, S.: A parameterization of evaporation from bare soil surfaces, J. Appl. Meteor., 29, 385–389, 1990.

Lafont, S., Zhao, Y., Calvet, J., Peylin, P., Ciais, P., Maignan, F. and Weiss, M.: Modelling LAI, surface water and carbon fluxes at high-resolution over France: comparison of ISBA-A-gs and ORCHIDEE, Biogeosciences, 9, 439–456, 2012.

Leuning, R., Van Gorsel,E., Massman, W.J., Isaac, P.R.: Reflections on the surface energy imbalance problem, Agr. Forest Meteorol., 156, 65-74, 2012.

Mahfouf, J. F. and Noilhan, J.: Comparative Study of Various Formulations of Evaporations from Bare Soil Using In Situ Data. J. Appl. Meteor., 30, 1354–1365, 1991.

Masson, V, Champeaux, J-L., Chauvin, F., Meriguet, C., Lacaze, R: A global database of land surface parameters at 1-km resolution in meteorological and climate models, J. Climate, 16, 1261–1282, 2003.

Masson, V., Le Moigne, P., Martin, E., Faroux, S., Alias, A., Alkama, R., Belamari, S., Barbu, A., Boone, A., Bouyssel, F., Brousseau, P., Brun, E., Calvet, J.-C., Carrer, D., Decharme, B., Delire, C., Donier, S., Essaouini, K., Gibelin, A.-L., Giordani, H., Habets, F., Jidane, M., Kerdraon, G., Kourzeneva, E., Lafaysse, M., Lafont, S., Lebeaupin Brossier, C., Lemonsu, A., Mahfouf, J.-F., Marguinaud, P., Mokhtari, M., Morin, S., Pigeon, G., Salgado, R., Seity, Y., Taillefer, F., Tanguy, G., Tulet, P., Vincendon, B., Vionnet, V., and Voldoire, A.: The SURFEXv7.2 land and ocean surface platform for coupled or offline simulation of earth surface variables and fluxes, Geosci. Model Dev., 6, 929-960, 2013.

Mauder, M., Cuntz, M., Drüe, C., Graf, A., Rebmann, C., Schmid, H.P., Schmidt, M., Steinbrecher, R.: A strategy for quality and uncertainty assessment of long-term eddy-covariance measurements, Agr. Forest Meteorol. 169, 122–135, 2013.

Merlin, O., Al Bitar, A., Rivalland, V., Béziat, P., Ceschia, E., Dedieu, G.: An Analytical Model of Evaporation Efficiency for Unsaturated Soil Surfaces with an Arbitrary Thickness, Journal of Applied Meteorology and Climatology, 50, 457–471, 2011.

Mertens J, Madsen H, Feyen L, Jacques D, Feyen J.: Including prior information and its relevance in the estimation of effective soil parameters in unsaturated zone modelling. Journal of Hydrology, 294, 251 – 269, 2004.

Mertens, J., Madsen, H., Kristensen, M., Jacques, D., Feyen, J.: Sensitivity of soil parameters in unsaturated zone modelling and the relation between effective, laboratory and in situ estimates, Hydrol. Process., 19, 1611–1633, 2005.

Montaldo, N., and Albertson, J D.: On the Use of the Force–Restore SVAT Model Formulation for Stratified Soils, J. Hydrometeorology, 2, 571-578, 2001.

Moureaux C., Ceschia, E., Arriga, N., Beziat, P., Eugster., Kutsch, W L., Pattey, E.: Eddy covariance measurements over crops, in Aubinet, M., Vesala, T., Papale, D., (Eds), Eddy Covariance: A practical guide to measurement and data analysis, 319-332, 2012.

Mueller, B., Seneviratne, S.I.: Systematic land climate and evapotranspiration biases in CMIP5 simulations, Geophysic Research Letters, 41, 128–134, 2014.

Noilhan, J. and Planton, S.:. A simple parameterization of land surface processes for meteorological models, Mon. Wea. Rev., 117, 536-549, 1989.

Noilhan, J. and Mahfouf, J.-F.: The ISBA land surface parameterisation scheme, Global and Planetary Change, 13, 145-159, 1996.

Noilhan, J., Donier, S., Sarrat, C., Moigne, P. L.: Regional-scale evaluation of a land surface scheme from atmospheric boundary layer observations, J. Geophys. Res., 116, 1-17, 2011.

Olioso, A., Carlson, T.N., and Brisson, N.:Simulation of diurnal transpiration and photosynthesis of a water stressed soybean crop. Agric. For. Meteorol. 81, 41–59, 1996.

~~Olioso, A., Chauki, H., Wigneron, J.-P., Bergaoui, K., Bertuzzi, P., Chanzy, A., Bessemoulin, P.,Calvet, J.-C.: Estimation of energy fluxes from thermal infrared, spectral reflectances,microwave data and SVAT modelling, Phys. Chem. Earth 24, 829–836, 1999.~~

Olioso, A., Chauki, H., Courault, D., and Wigneron, J.-P.: Estimation of Evapotranspiration and Photosynthesis by Assimilation of Remote Sensing Data into SVAT Models, Remote Sensing of Environment, Volume 68, 341-356, 1999.

Olioso, A., Braud, I., Chanzy, A., Courault, D., Demarty, J., Kergoat, L., Lewan, E., Ottlé, C., Prévot, L., Zhao, W.., Calvet, J.-C., Cayrol, P., Jongshaao, R., Moulin, S., Noilhan, J., Wigneron, J.-P.: SVAT modeling over the Alpilles-ReSeDA experiment: comparing SVAT models over wheat fields, Agronomie 22, 651–668, 2002.

Olioso, A., Inoue, Y., Ortega-FARIAS, S., Demarty, J., Wigneron, J.-P., Braud, I., Jacob, F., Lecharpentier, P., Ottle, C., Calvet, J.-C., Brisson, N.: Future directions for advanced

evapotranspiration modeling: Assimilation of remote sensing data into crop simulation models and SVAT models, Irrigation and Drainage Systems 19, 377–412, 2005.

Overgaard, J., Rosbjerg, D., Butts, M. B.: Land-surface modelling in hydrological perspective – a review, Biogeosciences, 3, 229-241, 2006.

Pitman, A. J.: The evolution of, and revolution in, land surface schemes designed for climate models, Int. J. Climatol., 23: 479–510. doi: 10.1002/joc.893, 2003.

Quintana-Seguí, P., Le Moigne, P., Durand, Y., Martin, E., Habets, F., Baillon, M., Canellas, C., Franchisteguy, L., Morel, S.: Analysis of Near-Surface Atmospheric Variables: Validation of the SAFRAN Analysis over France. Journal of Applied Meteorology and Climatology, 47, 92-107, 2008.

Rebmann, C., Kolle., O., Heinesch, B., Queck., R, Ibrom, A., Aubinet., M.: Data acquisition and flux calculation, in Aubinet, M., Vesala, T., Papale, D., (Eds), Eddy Covariance: A practical guide to measurement and data analysis, Springer, pp. 59-84, 2012.

Richardson, A.D., Hollinger, D.Y., Burba, G.G., Davis, K.J., Flanagan, L.B., Katul, G.G., William Munger, J., Ricciuto, D.M., Stoy, P.C., Suyker, A.E., Verma, S.B., Wofsy, S.C.: A multi-site analysis of random error in tower-based measurements of carbon and energy fluxes, Agr. Forest Meteorol., 136, 1–18, 2006.

Sellers, P. J., and Dorman, J. L.:: Testing the Simple Biosphere Model (SiB) Using Point Micrometeorological and Biophysical Data, J. Climate Appl. Meteor., 26, 622–651, 1987.

Schaap, M. G., Leij, F. J., and van Genuchten, M. T.: ROSETTA: a computer program for estimating soil hydraulic parameters with hierarchical pedotransfer functions, J. Hydrol., 251, 163– 176 , 2009.

Scharnagl, B., Vrugt, J. a., Vereecken, H., Herbst, M.: Inverse modelling of in situ soil water dynamics: investigating the effect of different prior distributions of the soil hydraulic parameters, Hydrol. Earth Syst. Sci., 15, 3043–3059, 2011.

Steenpass, C., Vanderborght, J., Herbst, M., Simonek, J., and Vereecken, H.: Estimating soil hydraulic properties from infrared measurements of soil surface temperatures and TDR data, Vadose Zone J., 9, 910–924,

Twine, T.E., Kustas, W.P., Norman, J.M., Cook, D.R., Houser, P.R., Meyers, T.P., Prueger, J.H., Starks, P.J., Wesely, M.L.: Correcting eddy-covariance flux underestimates over a grassland, Agr. Forest Meteorol., 103, 279–300, 2000.

Vereecken, H., Maes, J., and Darius, P.: Estimating the soil moisture retention characteristic from texture, bulk density and carbon content, Soil Sci., 148, 389–403, 1989.

Vidal, J.-P., Martin, E., Franchistéguy, L., Habets, F., Soubeyroux, J.-M., Blanchard, M., and Baillon, M: Multilevel and multiscale drought reanalysis over France with the Safran-Isba-Modcou hydrometeorological suite, Hydrol. Earth Syst. Sci., 14, 459-478, doi:10.5194/hess-14-459-2010, 2010.

Vrugt, J. a., Braak, C.J.F., Gupta, H. V., Robinson, B. a., 2008. Equifinality of formal (DREAM) and informal (GLUE) Bayesian approaches in hydrologic modeling ? Stoch. Environ. Res. Risk Assess. 23, 1011–1026.

Wetzel, P. J., and Chang, J. T.:Concerning the relationship between evapotranspiration and soil moisture, J. Climate Appl. Meteor., 26, 18–27, 1987.

Wilson, K., Goldstein, A., Falge, E., Aubinet, M., Baldocchi, D., Berbigier, P., Bernhofer, C., Ceulemans, R., Dolman, H., Field, C., Grelle, A., Ibrom, A., Law, B.E., Kowalski, A., Meyers, T., Moncrieff, J., Monson, R., Oechel, W., Tenhunen, J., Valentini, R., Verma, S.: Energy balance closure at FLUXNET sites, Agr. Forest Meteorol., 113, 223–243, 2002.

Workmann, S. R. and Skaggs, R. W.: Sensitivity of water management models to approaches for determining soil hydraulic properties, Transaction of the ASAE, 37(1), 95–102, 1994.

## Tables

### Table 1 : Definition of the main symbols

BIAS: Mean difference between simulated and measured values

EB: Energy balance

E: Soil evaporation (mm)

ET: Cumulative evapotranspiration (mm)

$ET_d$: Daily daytime evapotranspiration (mm $day^{-1}$)

G: Ground heat flux (W $m^{-2}$)

h: Matric potential (m)

H: Sensible heat flux (W $m^{-2}$)

K: Hydraulic conductivity (m $s^{-1}$)

$K_s$: Hydraulic conductivity at saturation (m $s^{-1}$)

LE: Latent heat flux (W $m^{-2}$)

MaxAWC: Maximum root-zone water stock available for the crop (mm)

Meas: Measurement

MD: Mean difference

PTF: Pedotransfer function

RN: Net radiation (W $m^{-2}$)

RMSE: root mean square error between simulated and measured values

RMSD: root mean square difference between two simulations or two measurements

SDD: standard deviation of the differences between two simulations or two measurements

T: transpiration flux (mm)

$Z_{root\text{-}zone}$: Rooting depth (m)

$\theta_{fc}$ : volumetric soil moisture at field capacity ($m^3\,m^{-3}$)

$\theta_{sat}$ : volumetric soil moisture at saturation ($m^3\,m^{-3}$)

$\theta_{wp}$ : volumetric soil moisture at wilting point ($m^3\,m^{-3}$)

$\theta_{surf}$ : superficial volumetric soil moisture (0-0.01m) ($m^3\,m^{-3}$)

$\theta_{root\text{-}zone}$: root-zone volumetric soil moisture (0-$d_2$) ($m^3\,m^{-3}$)

Table 2: 2001-2012 crop succession. The first sunflower in 2003 (1) was stopped and replaced by a new one. The 2009 maize (2) was stopped and replaced by sorghum because the emergence of maize was too heterogeneous. T and Rain are the mean temperature and cumulative precipitation, respectively, over the crop cycle.

| Year | Crop | Sowing date | Harvest date | Irrigation (mm) | Rain (mm) | T (°C) |
|---|---|---|---|---|---|---|
| 2001 | Maize | 2001/04/25 | 2001/09/28 | 375 | 232.0 | 20.7 |
| 2002 | Wheat | 2001/10/23 | 2002/07/02 | 0 | 399.0 | 11.6 |
| 2003 | Sunflower[1] | 2003/04/16 | 2003/05/26 | 40 | 68.0 | 17.1 |
| 2003 | Sunflower | 2003/06/02 | 2003/09/19 | 225 | 68.5 | 24.8 |
| 2004 | Wheat | 2003/11/07 | 2004/06/28 | 0 | 422.0 | 11.2 |
| 2005 | Peas | 2005/01/13 | 2005/06/22 | 100 | 203.5 | 11.9 |
| 2006 | Wheat | 2005/10/27 | 2006/06/27 | 20 | 256.0 | 10.7 |
| 2007 | Sorghum | 2007/05/10 | 2007/10/16 | 80 | 168.5 | 20.6 |
| 2008 | Wheat | 2007/11/13 | 2008/07/01 | 20 | 502.5 | 11.7 |
| 2009 | Maize[2] | 2009/04/23 | 2009/06/15 | 80 | 110.5 | 19.2 |
| 2009 | Sorghum | 2009/06/25 | 2009/09/22 | 245 | 89.0 | 23.6 |
| 2010 | Wheat | 2009/11/19 | 2010/07/13 | 0 | 446.5 | 11.6 |
| 2011 | Sorghum | 2011/04/22 | 2011/09/22 | 60 | 268.5 | 21.4 |
| 2012 | Wheat | 2011/10/19 | 2012/06/25 | 0 | 437.0 | 12.0 |

Table 3: Mean soil properties over the 0-1.2m soil profile. density is the soil bulk density. $\theta_s$ is the soil moisture at saturation derived from bulk density measurements. $\theta_{wp}$, $\theta_{fc}$ are the soil moisture at wilting point and field capacity, respectively. They were derived from the laboratory adjustment of the Brooks and Corey (1964) retention curve for given hydraulic conductivity (K) or matric potential (h) levels. The second and third rows represent the vertical ($\sigma_V$) and the spatio-temporal ($\sigma_{ST}$) variability of these measurements, respectively.

| | clay (%) | sand (%) | density (g cm$^{-3}$) | $\theta_s$ (m$^3$ m$^{-3}$) | $\theta_{wp}$ (h=-150 m) (m$^3$ m$^{-3}$) | $\theta_{fc}$ (h=-3.3 m) (m$^3$ m$^{-3}$) | $\theta_{fc}$ (K=0.1 mm day$^{-1}$) (m$^3$ m$^{-3}$) |
|---|---|---|---|---|---|---|---|
| **Mean** | **33.15** | **13.95** | **1.57** | **0.390** | **0.170** | **0.344** | **0.268** |
| $\sigma_V$ | 0.58 | 1.14 | 0.16 | 0.056 | 0.011 | 0.021 | 0.027 |
| $\sigma_{ST}$ | na | na | 0.05 | 0.019 | na | na | na |

Table 4: Estimates of the rooting depth ($Z_{root-zone}$), the soil moisture at field capacity ($\theta_{fc}$) and the soil moisture at wilting point ($\theta_{wp}$) derived from the time evolution of vertical profiles of field-measured soil moisture. MaxAWC (mm), defined as ($\theta_{fc}$-$\theta_{wp}$)* $Z_{root-zone}$ , represents the maximum root-zone water stock available for the crop. When no measurements were available, the mean value (*in italic*) from similar crop type was used. The last two rows are the mean and the standard deviation (std) computed over all crop cycles. The $Z_{root-zone}$=1.85 m obtained for wheat in 2006 can be related to the dryness of the crop period (256 mm of rain). The shallower $Z_{root-zone}$=1.0 m obtained for wheat in 2008 can be related to the wetness of the crop period (500 mm of rain).

| Crop | Year | $Z_{root-zone}$ (m) | $\theta_{fc}$ ($m^3 m^{-3}$) | $\theta_{wp}$ ($m^3 m^{-3}$) | MaxAWC (mm) |
|---|---|---|---|---|---|
| Maize | 2001 | 1.45 | 0.320 | 0.174 | 212 |
| Wheat | 2002 | 1.55 | 0.314 | 0.126 | 291 |
| Sunflower | 2003 | 1.80 | 0.311 | 0.209 | 184 |
| Wheat | 2004 | 1.65 | 0.314 | 0.183 | 216 |
| Peas | 2005 | 1.00 | 0.308 | 0.218 | 90.0 |
| Wheat | 2006 | 1.85 | 0.309 | 0.179 | 241 |
| Sorghum | 2007 | 1.65 | 0.306 | 0.183 | 203 |
| Wheat | 2008 | 1.00 | 0.279 | 0.202 | 77.0 |
| Maize | 2009 | *1.45* | *0.320* | *0.174* | *212* |
| Sorghum | 2009 | *1.65* | *0.306* | *0.183* | *203* |
| Wheat | 2010 | 1.75 | 0.327 | 0.182 | 254 |
| Sorghum | 2011 | *1.65* | *0.306* | *0.183* | *203* |
| Wheat | 2012 | *1.50* | *0.309* | *0.174* | *203* |
| mean | | 1.50 | 0.310 | 0.184 | 189 |
| std | | 0.30 | 0.012 | 0.025 | 56.0 |

Table 5: Values of the soil parameters used in the simulations. Sa corresponds to the standard implementation of the model achieved with the ECOCLIMAP-II rooting depth ($Z_{root-zone}$) and the ISBA pedotransfer estimates (1) of the wilting point ($\theta_{wp}$), the field capacity ($\theta_{fc}$) and the saturation ($\theta_s$). Distinct *in situ* estimates of these parameters are used in the Sb-Se simulations. They are defined as follows: (2): field-measured $\theta_s$; (3): laboratory retention curve estimate of $\theta_{fc}$ at h=-3.3m; (4): laboratory retention curve estimate of $\theta_{wp}$ at h=-150m; (5): laboratory retention curve estimate of $\theta_{fc}$ at K=0.1mm.day$^{-1}$; (6) : mean values of $Z_{root-zone}$, $\theta_{fc}$ and $\theta_{wp}$ estimated from the field measurements of soil moisture over the crop cycles; (7): CV: crop-varying values of $Z_{root-zone}$ and $\theta_{wp}$ estimated from the field measurement of soil moisture for each crop cycle (see Table 4). MawAWC is the the maximum root-zone water stock available for the crop.

| | Simulation cases | | | | |
|---|---|---|---|---|---|
| Soil parameters | Sa | Sb | Sc | Sd | Se |
| $\theta_{sat}$ ($m^3 m^{-3}$) | 0.479 (1) | 0.390 (2) | 0.390 (2) | 0.390 (2) | 0.390 (2) |
| $\theta_{fc}$ ($m^3 m^{-3}$) | 0.303 (1) | 0.344 (3) | 0.268 (5) | 0.310 (6) | 0.310 (6) |
| $\theta_{wp}$ ($m^3 m^{-3}$) | 0.214 (1) | 0.170 (4) | 0.170 (4) | 0.184 (6) | CV (7) |
| $Z_{root-zone}$ crop periods (m) | 1.5 | 1.5 (6) | 1.5 (6) | 1.5 (6) | CV (7) |
| MaxAWC (mm) | 134 | 261 | 147 | 189 | CV (7) |
| $Z_{root-zone}$ inter-crop periods (m) | 1.5 | 1.5 | 1.5 | 1.5 | 0.5 |

Table 6: Performances of the simulated energy fluxes for the simulation Sa. RN is the net radiation. H, LE and G are the sensible, latent and ground heat fluxes. The metrics were computed over the valid measurements available for each variable. For LE, only the 2004-2012 period is used. N and r are the number of samples and the correlation coefficient, respectively.

| RN (W $m^{-2}$) | | | | H (W $m^{-2}$) | | | | LE (W $m^{-2}$) | | | | G (W $m^{-2}$) | | | |
|---|---|---|---|---|---|---|---|---|---|---|---|---|---|---|---|
| N | r | RMSE | BIAS | N | r | RMSE | BIAS | N | r | RMSE | BIAS | N | r | RMSE | BIAS |
| 197255 | 0.99 | 27.7 | 0.2 | 103886 | 0.85 | 56.2 | 17.6 | 96214 | 0.80 | 52.4 | -11.8 | 191619 | 0.88 | 46.9 | -1.3 |

Table 7: Performances of simulated latent heat flux (LE), daily daytime evapotranspiration ($ET_d$) and root-zone soil moisture ($\theta_{root\text{-}zone}$) computed over the 20 November 2003-18 December 2012 period for which direct measurements of LE were available. $ET_d$ was computed when 90% of daytime measurements were valid for each day. Sa corresponds to the standard implementation of the model achieved with the pedotransfer estimates of the soil parameters. The rest of the simulations were achieved with distinct set of *in situ* soil parameters as defined in Table 5. N is the number of samples used to evaluate each variable. Meas is the mean value of the measured variable.

| | **CROP CYCLE** | | | | | | **INTER-CROP** | | | | | |
|---|---|---|---|---|---|---|---|---|---|---|---|---|
| | **LE (W m$^{-2}$)** | | **$ET_d$** (mm day$^{-1}$) | | **$\theta_{root\text{-}zone}$ (m$^3$ m$^{-3}$)** | | **LE (W m$^{-2}$)** | | **$ET_d$** (mm day$^{-1}$) | | **$\theta_{root\text{-}zone}$ (m$^3$ m$^{-3}$)** | |
| N | 52260 | | 944 | | 179 | | 43954 | | 853 | | 135 | |
| Meas | 70.1 | | 1.64 | | 0.255 | | 35.6 | | 0.85 | | 0.247 | |
| | RMSE | BIAS | RMSE | BIAS | RMSE | BIAS | RMSE | BIAS | RMSE | BIAS | RMSE | BIAS |
| **Sa** | 61.6 | -14.3 | 1.07 | -0.30 | 0.034 | 0.022 | 38.6 | -8.9 | 0.58 | -0.17 | 0.033 | 0.026 |
| **Sb** | 63.3 | 5.0 | 1.02 | 0.21 | 0.033 | 0.025 | 45.2 | 3.7 | 0.71 | 0.19 | 0.041 | 0.034 |
| **Sc** | 60.7 | -11.8 | 1.03 | -0.24 | 0.030 | -0.015 | 37.7 | -7.6 | 0.55 | -0.14 | 0.024 | -0.011 |
| **Sd** | 61.8 | - 0.3 | 1.00 | 0.07 | 0.024 | 0.012 | 40.7 | -0.2 | 0.60 | 0.06 | 0.026 | 0.017 |
| **Se** | 61.3 | 1.0 | 1.00 | 0.10 | 0.022 | 0.012 | 38.8 | -1.2 | 0.55 | 0.04 | 0.029 | 0.021 |

Table 8: Comparison of the direct measurement of LE (Direct), the energy balance residue estimate of LE (Residue) and the bowen ratio estimate of LE (Bowen). RMSD is the root mean square of the differences between the LE estimates. SDD is the SD of the differences between the LE estimates. For Y versus X, MD is computed as Y-X. In the last row, the MD in cumulative ET over 12-yr is computed relatively to X.

| | Bowen versus Direct | Residue versus Direct | Bowen versus Residue |
|---|---|---|---|
| RMSD ($W\ m^{-2}$) | 25.0 | 36.3 | 29.3 |
| SDD ($W\ m^{-2}$) | 23.9 | 36.2 | 28.9 |
| MD ($W\ m^{-2}$) | 7.5 | 3.2 | 4.3 |
| MD over 12-years (mm) | 727 | 310 | 417 |
| MD over 12-years (%) | 12 | 5 | 6.5 |

Table 9: Mean and standard deviation (SD) of the parameters used in the Monte-Carlo analysis. $g_m$ C3 and $g_m$ C4 denote the mesophyll conductance (gm in m $s^{-1}$ ) for C3 and C4 crop. $\theta_s$ ,, $\theta_{fc}$ , $\theta_{wp}$ are the soil moisture at saturation, at field capacity and at wilting point (**$m^3$ $m^{-3}$**). $Z_{root-zone}$ is the rooting depth (m). The mean values are those used in the simulation Sd. The standard deviation of the soil parameters correspond to their spatiotemporal variability reported in Table 3 &4. For gm, it is derived from literature meta-analysis (Calvet et al., 2000; Calvet et al., 2004).

| | $Z_{root-zone}$ | $\theta_{sat}$ | $\theta_{fc}$ | $\theta_{wp}$ | $g_m$ C3 | $g_m$ C4 |
|---|---|---|---|---|---|---|
| mean | 1.5 | 0.390 | 0.310 | .184 | 0.001 | 0.009 |
| SD | 0.3 | 0.019 | 0.012 | 0.025 | 0.0007 | 0.007 |

## Figures:

Figure 1: Illustration of the typical succession of winter and summer crop over the Avignon site. To represent the crop succession in the simulation, the 12 year period was split into sub-simulation periods corresponding to crop and inter-crop periods. The simulation was initialized once on 25 April 2001 using the *in situ* soil temperature and soil moisture measurements. To ensure the continuity between 2 contiguous sub-simulations, each sub-simulation was initialized using the simulated soil moisture (θ) and soil temperature (T) of the last time step of the previous sub-simulation.

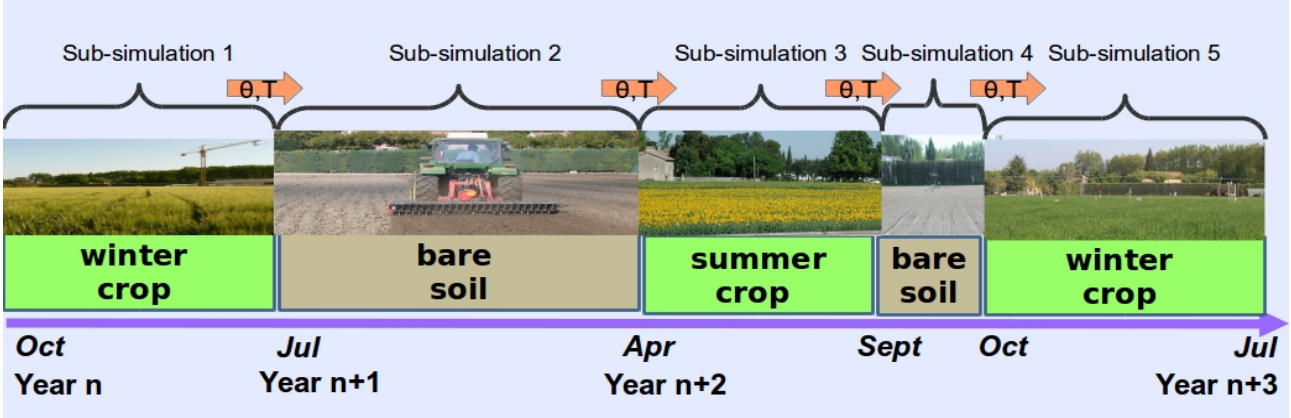

Fig. 2.: Evolution of simulated and measured evapotranspiration (ET in mm), simulated soil evaporation (E in mm), simulated plant transpiration (T in mm), simulated and measured daily daytime ET ($ET_d$ in mm), simulated and measured daily mean of root-zone soil moisture ($\theta_{root-zone}$ in $m^3$ $m^{-3}$), 10-d rainfall and irrigation (in mm), daily mean of *in situ* Leaf Area Index (LAI in $m^2$ m-2) over the 2001-2012 period. For clarity reasons, the average of daily values over 10 days are displayed. Cumulative values were computed over the time steps for which valid ET measurements were available. $ET_d$ was computed when 90% of valid daytime measurements were available for each day. The simulation corresponds to the standard implementation of the model (Sa). Crop and inter-crop periods are represented by grey and white background, respectively.

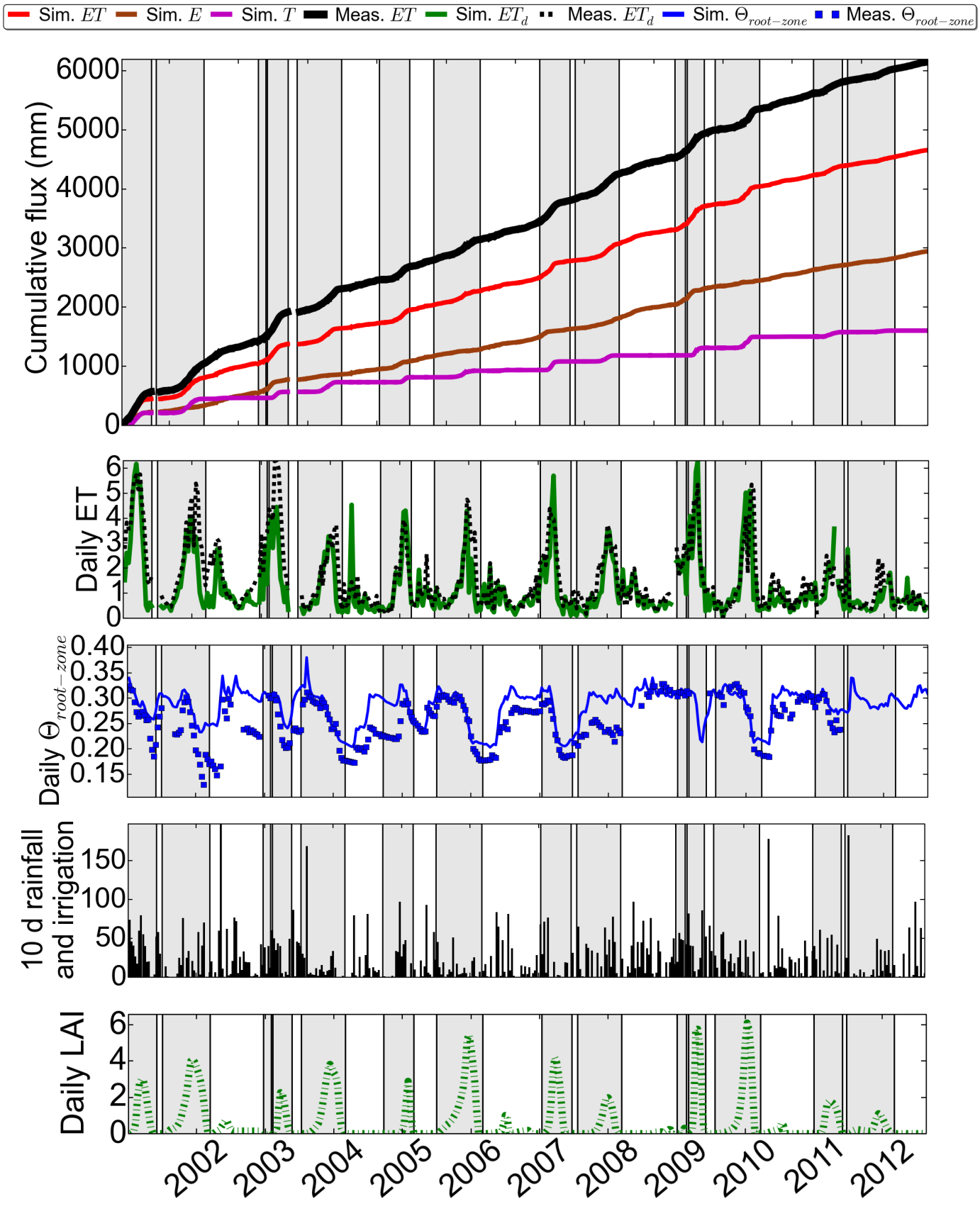
Sim. $ET$
Sim. $E$
Sim. $T$
Meas. $ET$
Sim. $ET_d$
Meas. $ET_d$
Sim. $\Theta_{root-zone}$
Meas. $\Theta_{root-zone}$
Cumulative flux (mm)
0
1000
2000
3000
4000
5000
6000
Daily ET
0
1
2
3
4
5
6
Daily $\Theta_{root-zone}$
0.15
0.20
0.25
0.30
0.35
0.40
10 d rainfall and irrigation
0
50
100
150
Daily LAI
0
2
4
6
2002
2003
2004
2005
2006
2007
2008
2009
2010
2011
2012

Fig. 3.: Evolution of (a) measured and simulated evapotranspiration (ET) and (b) measured and simulated root-zone soil moisture ($\theta_{root\text{-}zone}$), over the wheat cycle in 2006. Sa is the standard simulation achieved with the pedotransfer estimates of the soil parameters ($\theta_{wp}$=0.214) and the ECOCLIMAP-II value of $Z_{root\text{-}zone}$ (1.5 m). Sd was achieved with the average values of $\theta_{wp}$ (0.184) and $Z_{root\text{-}zone}$ (1.5 m) derived from the analysis of the soil moisture measurements over each crop cycle. Se was achieved with $\theta_{wp}$ (0.179) and $Z_{root\text{-}zone}$ (1.85 m) estimated from the analysis of the soil moisture measurements over the wheat cycle in 2006. In panel a, the simulated transpirations are represented by dashed lines. The LAI cycle is represented by green dash-dot lines. In panel b, measured $\theta_{root\text{-}zone}$ over a root-zone depth of 1.50 m and 1.85m are displayed.

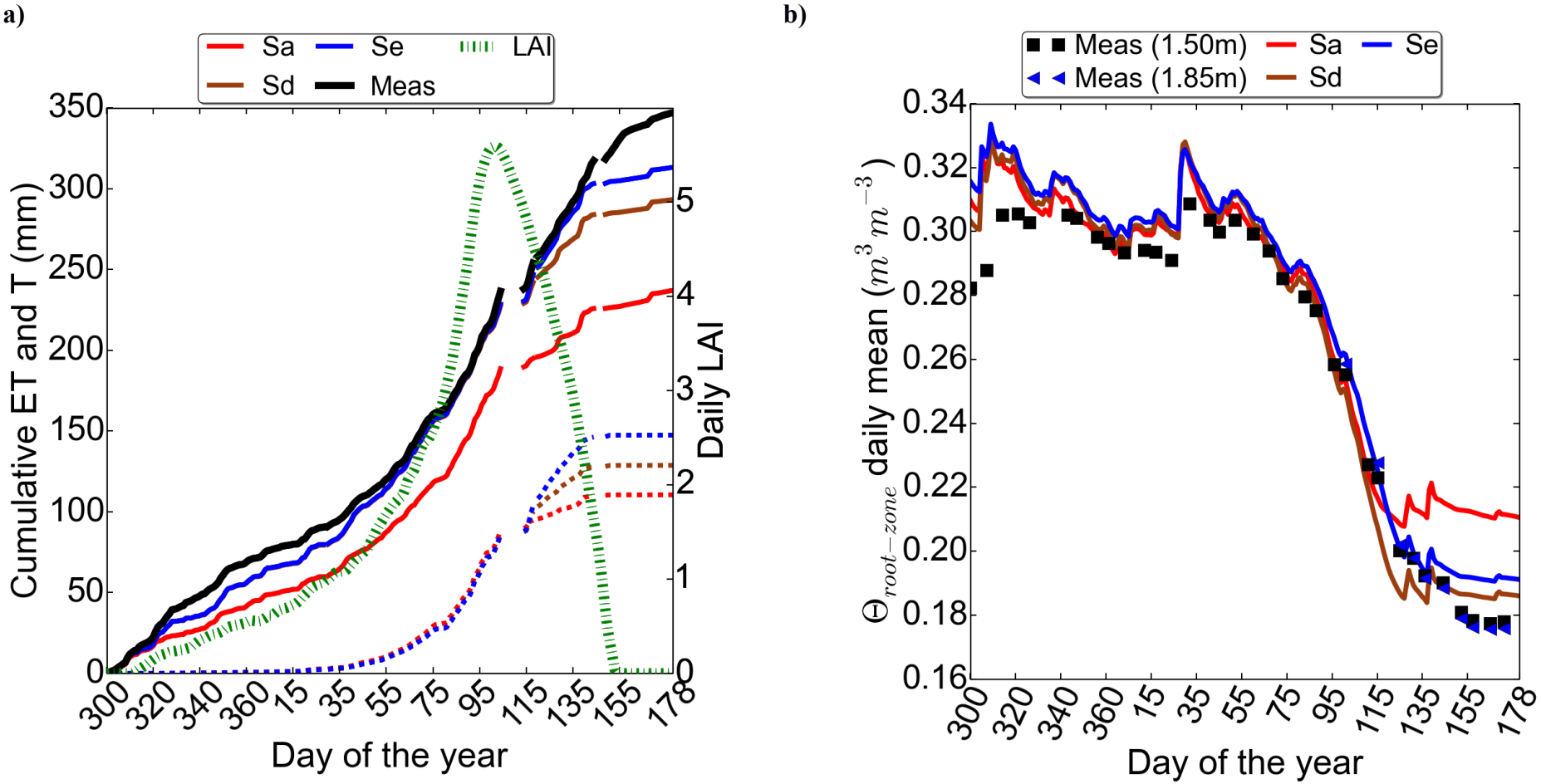

Fig. 4.: Evolution of (a) measured and simulated evapotranspiration (ET) and (b) measured and simulated root-zone soil moisture ($\theta_{root\text{-}zone}$), over the irrigated maize in 2001. Sa is the standard simulation based on the pedotransfer estimates of the soil parameters ($\theta_{rwp}$=0.214) and the ECOCLIMAP-II value of $Z_{root\text{-}zone}$ (1.5 m). Sd is achieved with the average values of $\theta_{wp}$ (0.184) and $Z_{root\text{-}zone}$ (1.5 m) derived from the analysis of the soil moisture measurements over each crop cycle. In panel a, the simulated transpirations are represented by dashed lines. The LAI cycle is represented by green dash-dot lines. In panel b, measured $\theta_{root\text{-}zone}$ over a root-zone depth of 1.50m is displayed.

a)

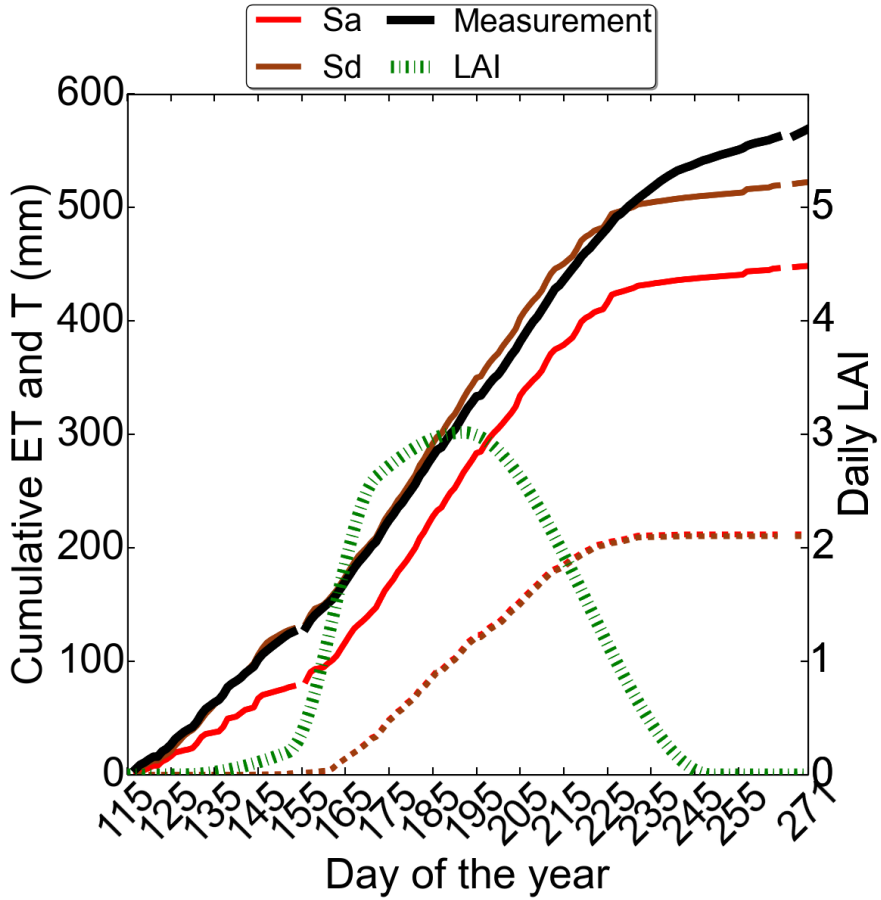


b)

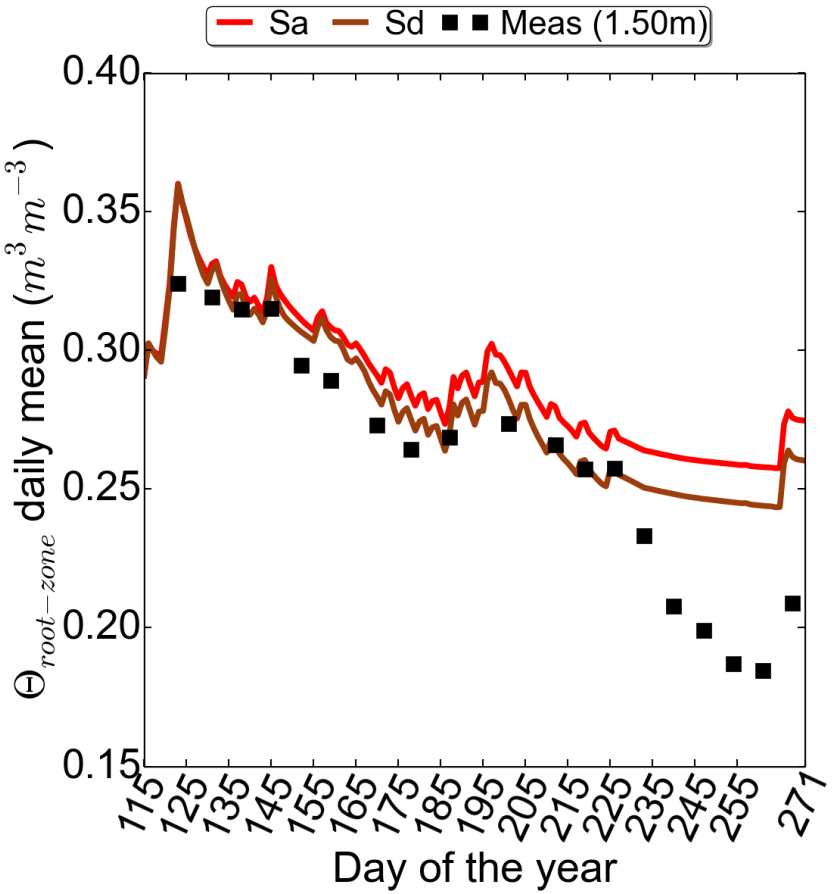

Fig. 5.: Evolution of (a) measured and simulated evapotranspiration (ET) and (b) measured and simulated root-zone soil moisture ($\theta_{root\text{-}zone}$), over the inter-crop period in 2010. ET corresponds to the soil evaporation since the soil is bare. Sa is the standard simulation based on the ISBA pedotransfer estimates of the soil parameters ($\theta_{fc}$=0.303 and $\theta_s$=0.479). Sb, Sc and Sd were achieved with the *in situ* estimate of $\theta_s$ (0.390). Sb and Sc were achieved with the laboratory retention curve estimates of $\theta_{fc}$ at h=-3.3m (0.344) and K=0.1 mm.d$^{-1}$(0.268), respectively. Sd and Se were achieved with $\theta_{fc}$ (0.310) derived from the field measured soil moistures. The soil reservoir depth $\theta_{root\text{-}zone}$ is equal to 1.5m in Sa, Sb, Sc, Sd and it is reduced to 0.5 m in Se. In panel b, measured $\theta_{root\text{-}zone}$ over a soil reservoir depth of 1.50 m and 0.50m are displayed.

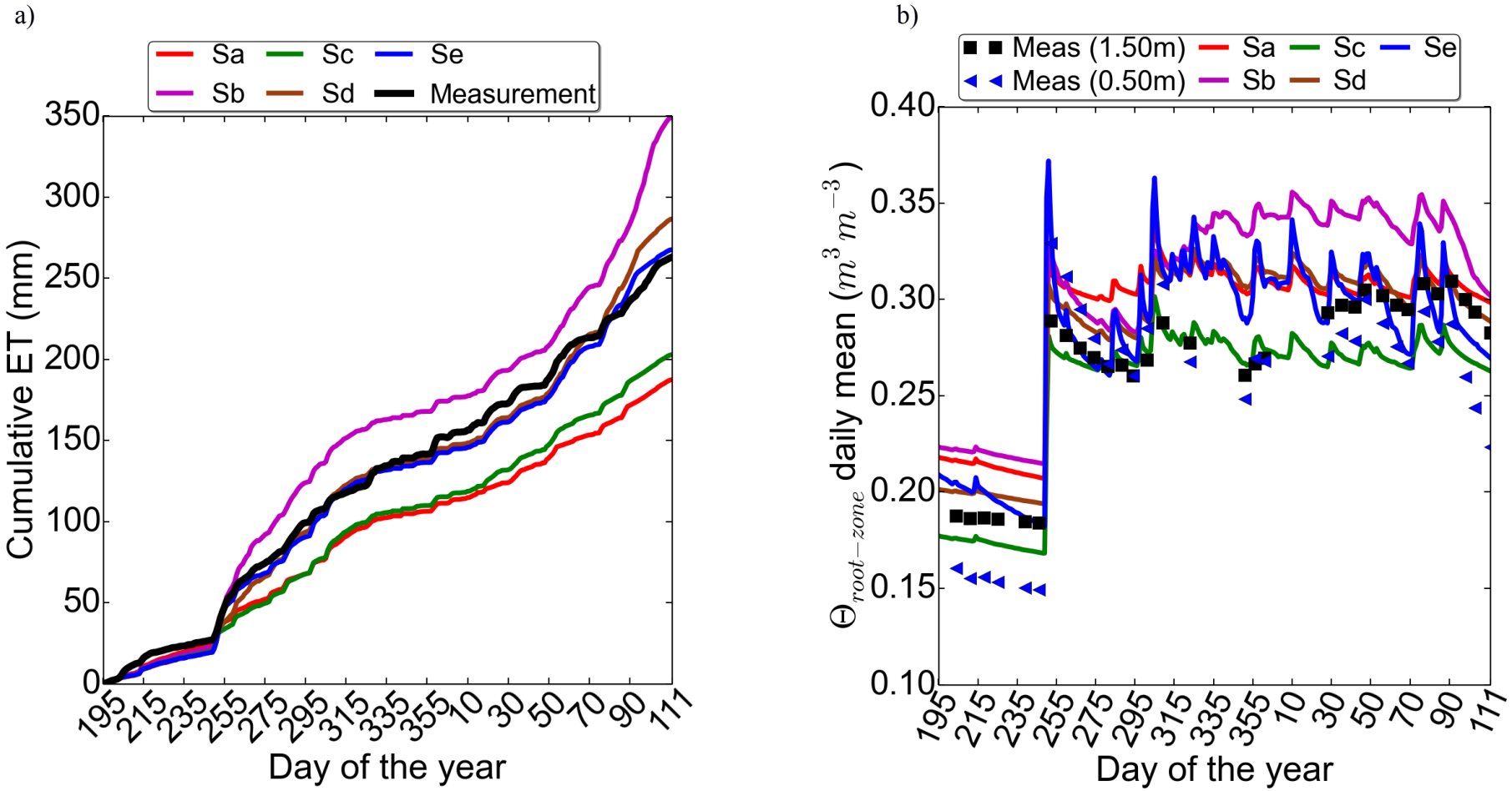

Fig. 6: Impact of the uncertainties in (a) the soil parameters ($Z_{root-zone}$, $\theta_s$ , $\theta_{fc}$ , $\theta_{wp}$) and (b) the mesophyll conductance, on simulated ET. The Sd simulation is achieved with the mean values of $Z_{root-zone}$, $\theta_s$ , $\theta_{fc}$ , $\theta_{wp}$ derived from the field measurements of soil moisture and the standard value of gm (Gibelin et al., 2006). The grey curves represent the 100 simulations generated by Monte-Carlo (MC). The 95% percentile interval (PI) of the MC simulations are computed over the empirical distributions of cumulative ET values.

a)

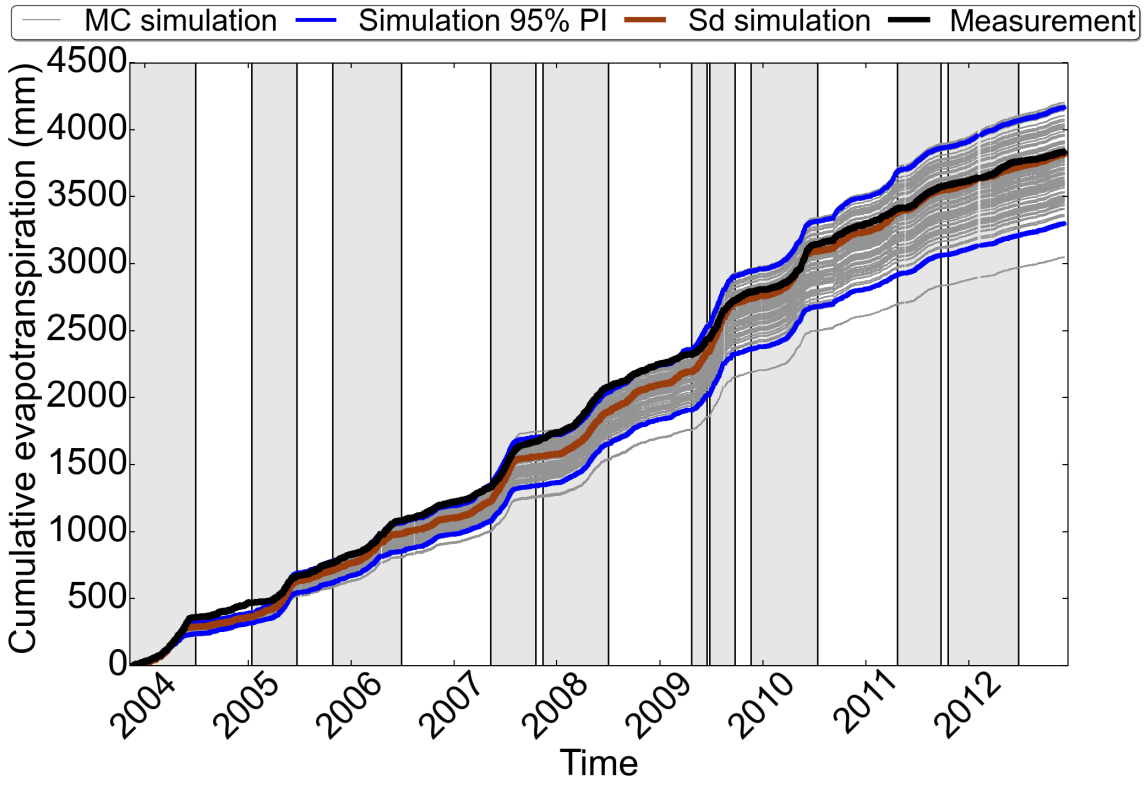
MC simulation
Simulation 95% PI
Sd simulation
Measurement
Cumulative evapotranspiration (mm)
0
500
1000
1500
2000
2500
3000
3500
4000
4500
2004
2005
2006
2007
2008
2009
2010
2011
2012
Time

b)

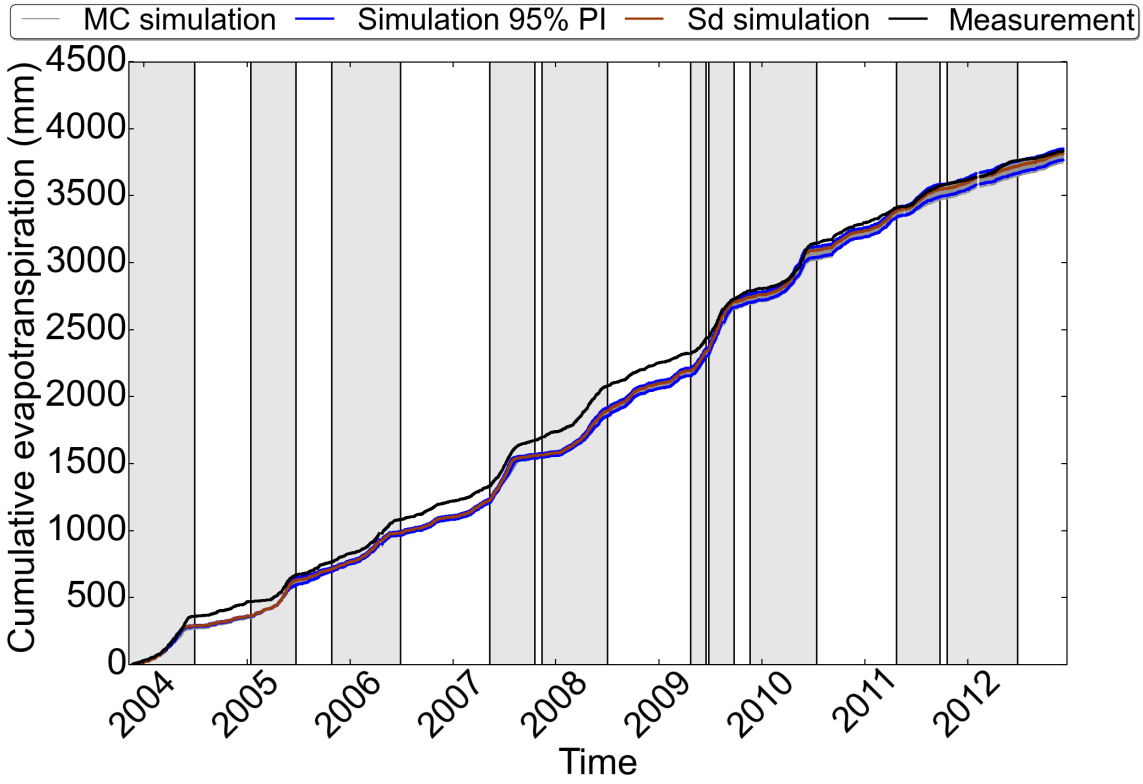
MC simulation
Simulation 95% PI
Sd simulation
Measurement
Cumulative evapotranspiration (mm)
0
500
1000
1500
2000
2500
3000
3500
4000
4500
2004
2005
2006
2007
2008
2009
2010
2011
2012
Time